

The Chemical Evolution of Globular Clusters - I. Reactive Elements and Non-Metals

A. Marcolini¹, B. K. Gibson¹, A. I. Karakas², P. Sánchez-Blázquez^{1,3}

¹*Jeremiah Horrocks Institute for Astrophysics & Supercomputing, University of Central Lancashire, Preston, PR1 2HE, UK*

²*Research School of Astronomy & Astrophysics, Mt Stromlo Observatory, Weston Creek ACT 2611, Australia*

³*Instituto de Astrofísica de Canaria; c/Vía Lactea s/n, E38205, La Laguna (Tenerife), Spain.*

Accepted ..., Received ...; in original ...

ABSTRACT

We propose a new chemical evolution model aimed at explaining the chemical properties of globular clusters (GC) stars. Our model depends upon the existence of (i) a peculiar pre-enrichment phase in the GC’s parent galaxy associated with very low-metallicity Type II supernovae (SNe II), and (ii) localized inhomogeneous enrichment from a single Type Ia supernova (SNe Ia) and intermediate-mass (4-7 M_{\odot}) asymptotic giant branch (AGB) field stars. GC formation is then assumed to take place within this chemically-peculiar region. Thus, in our model the first low-mass GC stars to form are those with peculiar abundances (i.e., O-depleted and Na-enhanced) while “normal” stars (i.e., O-rich and Na-depleted) are formed in a second stage when self-pollution from SNe II occurs and the peculiar pollution from the previous phase is dispersed. In this study, we focus on three different GCs: NGCs 6752, NGC 6205 (M 13) and NGC 2808. We demonstrate that, within this framework, a model can be constructed which is consistent with (i) the elemental abundance anti-correlations, (ii) isotopic abundance patterns, and (iii) the extreme [O/Fe] values observed in NGC 2808 and M 13, without violating the global constraints of approximately unimodal [Fe/H] and C+N+O.

Key words: nuclear reactions, nucleosynthesis, abundances - stars: abundances - stars: AGB and post-AGB - stars: chemically peculiar - globular clusters: individual: NGC 6752, NGC 6205, NGC 2808.

1 INTRODUCTION

As laboratories for both stellar and galactic physics, globular clusters (GCs) rank among the valuable tools available to astronomers. Ancient, co-eval, equidistant, and apparently mono-metallic, GCs give the appearance of being elegantly simple aggregates of stars. Behind this “mask of simplicity” though, lurks perplexing observations which have defied explanation for several decades.

First, each well-studied cluster to date shows star-to-star abundance variations of the light elements C, N, O, Na, Mg, and Al (Kraft 1994; Gratton et al. 2004, and references therein), not shared by field stars with similar metallicities (Gratton et al. 2000). These variations follow a common pattern with C-N, O-Na, and Mg-Al all anti-correlated (e.g Kraft et al. 1993; Grundahl et al. 2002; Cohen et al. 2002; Yong et al. 2003; Sneden et al. 2004; Yong et al. 2005; Cohen & Meléndez 2005; Carretta et al. 2006; Gratton et al. 2007; Marino et al. 2008). Importantly, the sum of C+N+O is observed to be approximately constant (e.g. Ivans et al. 1999; Carretta et al. 2005). More-

over, Smith et al. (2005) noted that stars in one of the Galactic globular clusters, NGC 6121, showed evidence for a Na-F anti-correlation, whereas Pasquini et al. (2005) and Bonifacio et al. (2007) found a Na-Li anti-correlation in NGC 6752 and 47 Tucanae, respectively. The abundances of Si, Ca, the iron-peak (e.g., Fe, Ni, and Cu) and neutron-capture elements (e.g., Ba, La, Eu) do not show the same star-to-star scatter, nor do they vary with the light elements (Gratton et al. 2004; James et al. 2004; Yong et al. 2006b, 2008). The most important exception to this is the most massive cluster ω Centauri, that shows both, a spread in age and [Fe/H], and a rise in s-process element abundances with increasing [Fe/H]. Evidence for ω Cen suggests it may have an extragalactic origin (e.g. Majewski et al. 2000; Smith et al. 2000; Gnedin et al. 2002; Bekki & Freeman 2003; Romano et al. 2007; Marcolini et al. 2007).

The above abundance trends have been found for stars in all evolutionary phases, from the main-sequence turn-off through to the tip of the first giant branch, which has lent support to the “self-pollution” hypothesis

(Cottrell & Da Costa 1981; Dantona et al. 1983). This is in contrast to deep mixing, where the abundance anomalies are produced by internal mixing during the ascent of the giant branch, after the first dredge-up (Sweigart & Mengel 1979; Pinsonneault 1997; Charbonnel 1994). Further evidence for self-pollution comes from a lack of variation in the O-Na and Mg-Al anti-correlations with luminosity as the stars ascend the first giant branch.

According to the self-pollution scenario a previous generation of stars "contaminated" the atmospheres of stars observed today in GCs, or provided much of the material from which those stars formed (e.g. Jehin et al. 1998; Parmentier et al. 1999; Tsujimoto et al. 2007). The roughly constant $[\text{Fe}/\text{H}]$ abundances in a given GC led to the assumption that the polluters were low-metallicity, intermediate-mass asymptotic giant branch (AGB) stars, with masses between ~ 4 and $7 M_{\odot}$ (D'Antona & Caloi 2004; Bekki et al. 2007). The hot bottom burning experienced by these stars provides the hydrogen burning environment (at least qualitatively) that can alter the abundances of the light elements. Detailed AGB models have mostly failed to explain the observed abundance trends (Denissenkov & Herwig 2003; Fenner et al. 2004; Cohen & Meléndez 2005; Karakas et al. 2006a), but model uncertainties, including convection and mass loss, render predictions uncertain (Ventura & D'Antona 2005a,b). Recently, slow-winds from rotating massive stars (Prantzos & Charbonnel 2006; Smith 2006; Decressin et al. 2007) have also been proposed as another possible source of the abundance anomalies.

The canonical AGB enrichment scenario consists of two stages in which the first stars to form are those pre-polluted by core collapse supernovae (SNe II), and have $[\text{O}/\text{Fe}] \sim 0.5$ and $[\text{Na}/\text{Fe}] \sim -0.1$. After the first SNe II have driven away the gas from the proto-cluster, gas polluted by AGB winds starts to accumulate at the centre of the cluster and a second generation of stars with peculiar abundances can form. These second-generation stars will have depleted F and O, along with enhanced in N and Na with respect to the first generation. Variations to this scenario include (1) the AGB ejecta-enriched gas is also accreted on to the surface of some (e.g., segregated) stars (Parmentier et al. 1999), and (2) the AGB pollution comes, not only from the first generation of stars, but also from all AGB stars of the satellite galaxy where the GC is forming (Bekki et al. 2007). The second assumption was made to allow for a larger reservoir of material for the formation of the second generation of stars (Bekki & Norris 2006), as if all AGB pollution comes from the first generation of stars, is very difficult to explain the high fraction (as high as 50%) of peculiar-to-normal stars in GCs (e.g., D'Antona & Caloi 2004; D'Antona et al. 2005; Carretta et al. 2006; Piotto et al. 2007). The same results can be achieved by assuming that the GCs were much more massive in the past (by a factor of ~ 10 - $100\times$) and lost preferentially most (90-99%) of their first generation of stars through tidal interactions with the Milky Way (MW; e.g. D'Ercole et al. 2008).

Another way to solve the problems associated with the AGB-"pre-pollution" scenario is to assume that the polluters were not AGB stars but Type Ia supernovae. Marcolini et al. (2006) suggested that the O-depleted stars observed in dwarf spheroidal galaxies (dSphs) as well as in

the peculiar globular cluster ω Cen (Marcolini et al. 2007) can be explained if those stars were born in a small iron-rich volume *inhomogeneously* polluted by a single SN Ia. The ejecta of SNe Ia is very rich in Fe and extremely poor in O (compared to SNe II) thus stars forming in such confined regions would show very low values of $[\text{O}/\text{Fe}]$ (usually up to ~ -0.5). Dwarf galaxies, however, show a large spread (1.5 dex) of $[\text{Fe}/\text{H}]$, hence it is not clear if this model is applicable to the problem of the abundance anomalies in mono-metallic GCs.

In this paper we present a GC chemical evolution model where all of the observed chemical peculiarities arise from the inhomogeneous pollution of a single SN Ia and intermediate-mass AGB stars. This pollution is mixed with gas that was pre-enriched by very low-metallicity SNe II. Since each of these so-called "polluters" precede the formation of the GC itself, we call this type of enrichment "external pollution" (according to Bekki et al. 2007) from the Milky Way (or host galaxy). When the first stars with peculiar abundances are forming, SNe II start to explode, self-polluting the ISM and dispersing the inhomogeneous region. As star formation proceeds, the abundances of the forming stars will move from "peculiar" to "normal", where normal in this context means stars with chemical properties typical of SNe II enrichment. Eventually, the SNe II explosions will cease any further star formation (SF) and the GC will evolve passively. In previous studies, SN Ia had been discarded as polluters because the $[\text{Fe}/\text{H}]$ is essentially constant within a given GC, and SN Ia are efficient producers of iron. Nevertheless, we will show that our model is able to reproduce the observed anti-correlations, while keeping the iron content of the newly forming stars approximately constant.

In the following we test our scenario on a GC with a typical $[\text{O}/\text{Fe}]$ -depletion pattern (on the order of ~ -0.5), similar to the well-studied cluster NGC 6752 ($[\text{Fe}/\text{H}] = -1.56$). In addition we test our scenario on a more extreme case such as that of NGC 2808 ($[\text{Fe}/\text{H}] = -1.15$) and M 13 ($[\text{Fe}/\text{H}] = -1.50$) (Harris 1996), with $[\text{O}/\text{Fe}]$ -depletions as large as 1 dex.

2 INITIAL CONDITIONS

It is generally assumed that GCs were assembled during the formation of the Milky Way halo (or their parent galaxy) even though their chemical properties differ from those halo field stars of the same metallicity (e.g., Gratton et al. 2000; Freeman & Bland-Hawthorn 2002). It is likely that part, or all, of this difference can be traced to the very different conditions experienced by the respective systems e.g., deeper potential wells and the associated burst of SF.

Following this framework, we assume that a typical GC forms initially within gas pre-enriched by field polluters such as SNe II, but also from SNe Ia and AGB stars associated with (parent) halo star formation. However, due to the early stage of the formation of the halo (with respect to the rest of the parent/Milky Way), SNe Ia and AGB stars are not important in shaping the *mean* chemical properties of the gas unless they are polluting it inhomogeneously (i.e., polluting a small localized region). Thus, we assume that a typical GC will form initially in a peculiar region of the halo that was pre-polluted by SNe II, and in which the inhomogeneous pol-

lution of a single SN Ia and intermediate-mass AGB stars is added. In our model, all the chemical peculiarities observed in GC stars (i.e., O-depleted and Na-rich stars) which are not shared by their field counterparts arise due to this peculiar localized inhomogeneous pollution.

A schematic representation of how these initial conditions can be achieved is shown in Fig 1. According to our model, AGB material is deposited in the vicinity of a SNe Ia progenitor binary system. As the secondary explodes as a SN Ia and the supernovae remnant (SNR) expands, it will collect this surrounding AGB material in its shell. The numerical evolution of a radiative SNR has been analyzed in detail by Cioffi et al. (1988) and Thornton et al. (1998). These studies found that for normal ambient gas density of $n_0 = 1 - 10 \text{ cm}^{-3}$, the evolution of a SNR lasts for a few Myrs and that it reaches radius of $\sim 50\text{-}90 \text{ pc}$ (with the larger radii achieved for the smaller ambient gas densities). After radiating away most of its energy, the remnant will first stall, lose its identity and then collapse back (e.g. Slavin & Cox 1992, ; approximately after $R_{\text{max}}/c_s \sim 5\text{-}9 \text{ Myr}$, assuming an ambient sound speed c_s of 10 km s^{-1}). The result of this evolution will be a localized region of the halo, polluted inhomogeneously with SN Ia and AGB ejecta. These will be the initial conditions of our model which we define as the “pre-peculiar enrichment” scenario; we assume that the proto-GC starts forming stars in this peculiar region.

Regions polluted inhomogeneously by SNe Ia arise naturally in the hydrodynamical simulations of dSphs chemical enrichment performed by Marcolini et al. (2006, 2008). Cescutti (2008) also showed that a model which takes into account inhomogeneous pollution is able to explain the observed spread in s - and r -process elements at low metallicities in the Galactic halo (see also Ishimaru & Wanaajo 1999; Argast et al. 2000). Since both the peak SNe Ia rate (Matteucci & Recchi 2001; Mannucci et al. 2006) and the lifetime of a low-metallicity $5 M_{\odot}$ star (e.g., Schaller et al. 1992; Karakas & Lattanzio 2007) are comparable ($\sim 80 - 100 \text{ Myr}$), this apparently peculiar enrichment scenario seems reasonable. Mannucci et al. (2006) proposed that half of the SNe Ia associated with a starburst should explode on a timescale of the order $\sim 100 \text{ Myr}$. Marcolini et al. (2006,2008) have shown that even if a timescale greater than $1\text{-}2 \text{ Gyr}$ is needed to appreciate the cumulative effect of SNe Ia in the mean $[\alpha/\text{Fe}]$ ratio of spheroidal galaxies, the effect of a single SN Ia inhomogeneously polluting the ISM could be important in the first few hundred Myrs (see also Marcolini et al. 2007, for an application of this scenario to the particular case of $\omega \text{ Cen}$).

3 TWO-REGION MODEL

Our model is based on what could be termed a “two-region” chemical evolution framework with a simplified prescription for the chemical enrichment. As a first attempt to reproduce the main chemical properties of GC stars, we do not follow the ejecta of different mass progenitors, but we use IMF-averaged yields for both intermediate-mass AGB stars and SNe ejecta (see 4 for more detail). A sketch of the model is shown in Fig. 2, where the two regions – “inner” and “external” – are shown. The dark blue “inner region” in Fig. 2 corresponds initially to the blue-green circle in the

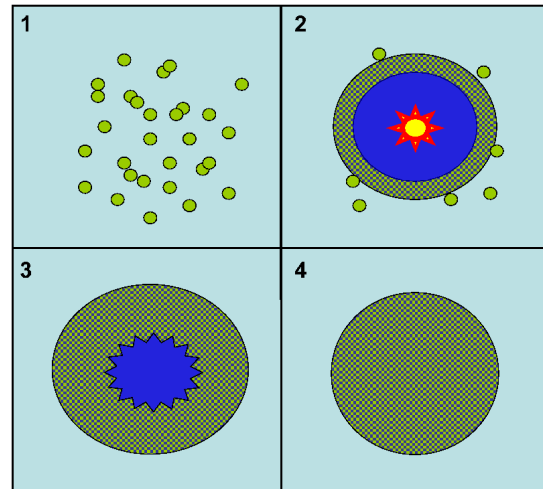


Figure 1. Schematic framework leading to the initial conditions required for our model: 1) low-metallicity $4\text{-}7 M_{\odot}$ AGB stars (green dots) start polluting a particular region of the halo which has been pre-enriched by SNe II; 2) a SN Ia explodes near this region and during its expansion collects the AGB material in its shell; 3) the SN remnant radiates away its energy and the gas starts re-collapsing, mixing the SN Ia ejecta with material from the AGB stars; 4) the final result is a peculiar region in the Galactic halo, where on top of the mean pre-enrichment from early SNe II, the inhomogeneous contribution by a single SN Ia and a number of intermediate-mass AGB stars is added. These are our assumed initial conditions for proto-GC formation. Note that the light-blue background volume (mainly polluted by early-SNe II) represents the mean chemical properties of the gas out of which “normal” field halo stars are formed.

last panel of Fig. 1 polluted inhomogeneously by a SN Ia and intermediate-mass AGB material; we will assume that the SF related to the GC formation only takes place inside this region. In the following, we will use the term “inhomogeneous pollution” to denote that this region has different chemical properties from the surrounding medium (note that the chemical properties inside the inner region itself are homogeneous).

The external region is simply described by the initial value of $[\text{Fe}/\text{H}]_{\text{ISM}}$ given in Table 1, which should reflect the mean chemical properties of the proto-halo gas at the epoch of GC formation (enriched mainly by SNe II). The inner region is initially described by its radius (R_{in} i.e., the degree to which the SN Ia was initially confined) and the mean chemical properties within, which is set by the number of $4\text{-}7 M_{\odot}$ AGB stars, N_{AGB} . Since most of the iron in the inner region is provided by a single SN Ia the value of R_{in} also defines the value of $[\text{Fe}/\text{H}]_{\text{in}}$ in the inner region. It is obvious that the localized iron-rich ejecta from the SN Ia will substantially increase the value of $[\text{Fe}/\text{H}]$ inside the inner region compared to the value in the external region, whereas intermediate-mass AGB stars increase the N, Na, the neutron-rich Mg isotopes and, possibly, Al. A glance at Table 1 shows that the inner region is a factor of $\sim 10 - 100$ more $[\text{Fe}/\text{H}]$ rich than the external ISM and also has a similar higher overall metallicity. For this reason the first generation of stars will be born with peculiar chemical properties: they will be depleted in O and Mg (because of the single

Table 1. Initial conditions of the model. Note that only three of the parameters are free as the value of $[\text{Fe}/\text{H}]_{\text{in}}$ is defined by R_{in} (see text for more details).

Model	$[\text{Fe}/\text{H}]_{\text{ISM}}$	$[\text{Fe}/\text{H}]_{\text{in}}$	R_{in} (pc)	N_{AGB}
NGC 6752	-2.55	-1.60	36	250
M 13	-3.50	-1.50	31	170
NGC 2808	-2.85	-1.10	24	180

SN Ia) and they will be enhanced in N, Na, and Al (due to AGB pollution). Note that in canonical AGB self-pollution models (e.g. Fenner et al. 2004) these stars are the last to form. While a detailed discussion about each element will be presented in the following sections, here we would like to point out that, in general, the trend for SN Ia is to decrease the $[X_i/\text{Fe}]$ value when X_i is not (or negligibly) produced in intermediate-mass AGB stars (e.g., O and the elemental Mg abundance to a lesser extent). In the case when the elements are overproduced in AGB stars (e.g., N, Na and, possibly, Al), the effect of the SN Ia is to mitigate their enhancement.

We assume that the star formation takes place only inside the inner region. As the SF proceeds, massive stars ($M_{\odot} \geq 8 M_{\odot}$) start exploding (as early as $\sim 3 - 4$ Myr after the onset of star formation Schaller et al. 1992) as SNe II, ejecting freshly synthesized metals. We assume that after each SN II explosion the inner region expands, driven by the explosions themselves, mixing the inner-region gas with the surrounding ISM, while the SF is still proceeding inside this region. During the evolution, we simply assume that the density remains constant and thus the mass inside a fixed radius is $M = \frac{4}{3}\pi\rho_0 R^3$. For each of the proposed GC models we assume a density of $\rho_0 = 4 \times 10^{-24}$ g cm $^{-3}$ which, for example, corresponds to a total mass of $M_{\text{ISM}} \simeq 3 \times 10^7 M_{\odot}$ inside a 500 pc radius sphere. Even if we were to assume a lower SF efficiency, there would still be more than sufficient gas to form a typical GC.

The simple relations governing the evolution after each SN II explosion can be summarized as:

$$R(t + \Delta t) = R(t) \times f_{\text{exp}} \quad (1)$$

$$X_i(t + \Delta t) = X_i(t) + X_i(\Delta R) + \langle X_i(\text{SNII}) \rangle \quad (2)$$

where f_{exp} is a constant governing the logarithmic expansion of the inner region after the explosion of every single SN II, Δt is the time interval between two successive SNe II explosions, $X_i(t)$ is the mass fraction of an element X at a time t within the radius $R(t)$, $X_i(\Delta R)$ is the mass fraction of an element X initially present in the corona $R(t+1) - R(t)$, and finally, $\langle X_i(\text{SNII}) \rangle$ is the average mass fraction of element X_i ejected by a single SN II (see Sec. 4). For example, the evolution of the $[\text{Fe}/\text{H}]$ abundance in the inner region at a time $(t + \Delta t)$ (where Δt is the time between two successive SNe II) is computed by adding the Fe initially present in this region at $R(t)$ to the iron ejected by the newly exploding SNe II and to the iron initially present in the external region $R(t + \Delta t) - R(t)$. This number is then divided by the total amount of hydrogen inside the new radius $R(t + \Delta t)$. All the other variables are calculated accordingly. We assume that this expansion is described by a logarithm law with a free parameter (usually of the order of $f_{\text{exp}} \sim 1.001$)

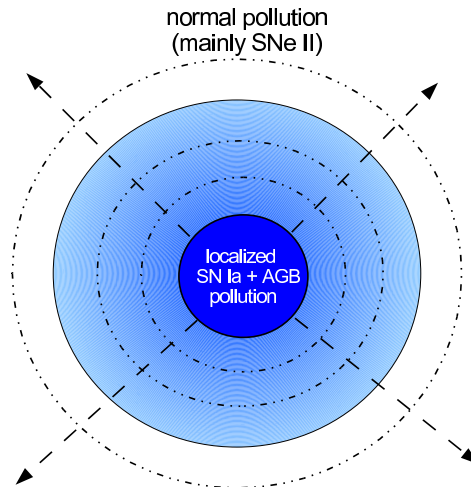


Figure 2. Schematic of the model. Initially, a localised volume (inner blue region) arises with the pollution from a single SN Ia and multiple intermediate-mass AGB stars. After a new generation of stars is born the associated SNe II begin to pollute and expand the inner volume, as well as mix it with the surrounding lower- $[\text{Fe}/\text{H}]$ interstellar medium.

which fixes the increase of $R(t)$ after each SN II explosion (i.e., $R(t + \Delta t) = R(t) \times f_{\text{exp}}$).

In Fig. 2 the dashed lines represent a sketch of the evolution of the inner region and the fact that the initial contribution of the single SN Ia (as well as AGB stars) is diluted during its expansion and the subsequent mixing with the outer, lower metallicity ISM. As soon as the first SNe II start to explode there are two contrasting mechanisms shaping the chemical properties of the newly forming stars. First, the freshly ejected SNe II metals directly pollute the gas where new stars are forming. Second, the inner volume is expanding and the gas inside this region is mixed with lower metallicity material. In Sec. 5.1 we will show that, during the chemical evolution process, it is possible to keep the $[\text{Fe}/\text{H}]$ abundance constant in the inner region (where the new stars are forming) owing to these two contrasting mechanisms.

While stars with peculiar properties form during the first stage, during the second stage the chemical properties of the forming stars α -enhanced) as SNe II start exploding. Marcolini et al. (2006) showed, for the specific case of dwarf galaxies, that even if a single SN Ia can temporarily pollute a small volume and dramatically change its chemical composition, its imprint disappears almost completely once the gas inside this volume mixes with the ISM. In the next section we will show that the last stars forming in our model (stars with $[\text{O}/\text{Fe}] \sim 0.5$) do not show any signature of the former AGB or SN Ia pollution, having chemical properties typical of pure SNe II ejecta.

We will also show, in Sec. 5.1, that in our model the inner region is more metal rich than the outer region and, accordingly, the cooling is much more efficient there. Therefore, this region is more likely to host an extremely enhanced SF – typical of GCs – than the outer ISM (where normal halo stars are forming).

Numerous authors have discussed, from an energetic perspective, the possibility that stellar clusters can

Table 2. Mean SNe II stellar yields averaged over the progenitor mass range 10–60 M_{\odot} for a Salpeter IMF and for different authors: W&W=Woosley & Weaver (1995); C&L=Chieffi & Limongi (2004); KOB=Kobayashi et al. (2006). The yields of Fe and He are given in solar masses while for different elements we show the $[X_i/\text{Fe}]$ ratios.

SNe II model	Fe	He	[C/Fe]	[N/Fe]	[O/Fe]	[Na/Fe]	[Mg/Fe]	[Al/Fe]
W&W (Z=0.0002)	6.1e-2	6.7	0.13	-1.73	0.51	-0.39	0.15	-0.24
W&W (Z=0.002)	6.9e-2	6.6	0.07	-0.86	0.46	-0.16	0.16	-0.04
C&L (Z=0.0001)	1.0e-1	5.7	0.41	-1.91	0.63	0.05	0.61	-0.14
C&L (Z=0.001)	1.0e-1	5.7	0.40	-0.96	0.63	0.26	0.61	0.11
KOB (Z=0.001)	7.5e-2	5.7	-0.16	-0.80	0.64	0.05	0.63	0.15
KOB (Z=0.001+HN)	9.3e-2	5.7	-0.26	-0.89	0.52	-0.08	0.52	0.28
Model (SNe II)	9.0e-2	6.0	-0.10	-0.90	0.50	-0.20	0.50	-0.10

experience SNe II self-enrichment, and there is a wide range of evidence as to whether, and to what extent, this is possible in GCs (e.g. Dopita & Smith 1986; Morgan & Lake 1989; Smith 1996; Parmentier & Gilmore 2001; Gnedin et al. 2002; Thoul et al. 2002; Parmentier 2004; Recchi & Danziger 2005; Prantzos & Charbonnel 2006). For example, it has been suggested that stellar winds and SNe explosions from the first generation of stars can form a metal-enriched supershell, where further star formation is triggered (Brown et al. 1991, 1995; Thoul et al. 2002; Parmentier 2004; Recchi & Danziger 2005). Brown et al. (1991) concluded that a small entirely self-enriched system of stars typically achieves a metallicity in the range $10^{-2} - 10^{-1} Z_{\odot}$, and that the second generation of stars would be expected to be extremely homogeneous in composition. Melioli & de Gouveia Dal Pino (2004) studied in detail the heating efficiency (i.e., the fraction of SNe energy which is not radiated away) of SNe exploding in a starburst environment with properties similar to that of our model. These authors found that the heating efficiency can be very close to zero (i.e., all the SNe energy is efficiently radiated away) for, up to, a few tens of Myr, before rapidly increasing to unity and leading to a possible galactic wind. While we cannot follow the dynamical evolution (and the energetics) of our model, it is possible to speculate that this second stage of star formation could be as rapid as $\sim 20 - 40$ Myr (with SNe II directly polluting the newly forming stars), or it could proceed in a long series of weak bursts if the star formation is self-regulated - i.e., the gas is temporarily expelled out of the star forming regions by the SNe and re-collapses (due to the outer pressure) once the SNe II energy is radiated away. If the star formation is self-regulated, the SF history can be as long as ~ 100 Myr. A longer SF history would require the contribution of AGB and SNe Ia self-pollution, which does not seem to be required in our model, to explain the chemical properties of GCs. Finally, in our case, the formation of a galactic wind would be associated with the cessation of the SF itself and it would happen after $\sim 1 - 5 \times 10^3$ SNe II explosions, depending upon the details of the model. Although these earlier studies seem to support the formation of second generation of stars after the occurrence of an explosive event, and the formation of a bound system, hydrodynamical simulations of the SNe II self-enrichment phase in quantitative detail are needed to further quantify the star-formation timescales and the viability of our model from a dynamical point of view. These will be presented in a forthcoming paper in this series.

4 YIELDS

As noted earlier we used IMF-averaged yields for both SNe II and intermediate AGB polluters. For SNe II, we explore the effect of using yields computed by different authors (Woosley & Weaver 1995; Chieffi & Limongi 2004; Kobayashi et al. 2006, see Table 2) and use the limits 10–60 M_{\odot} . Previous studies have found that the Woosley & Weaver (1995) models tend to overproduce the amount of Fe – with a subsequent underestimation of the $[\alpha/\text{Fe}]$ abundances – for this reason we half Fe values as done in several studies (e.g., Timmes et al. 1995; Goswami & Prantzos 2000; Fenner et al. 2004). While the set of yields are in reasonable agreement with one another for most of the elements, occasional differences as large as 0.4 dex are present (e.g., Gibson et al. 1997). We computed a set of yields that we use throughout the paper unless stated otherwise. These yields are the average value of the above mentioned theoretical set of yields when the agreement between them is good (when they differ less than 0.4 dex). Otherwise, we chose the yields that best reproduce the low metallicity ($-2.0 \leq [\text{Fe}/\text{H}] \leq -1.0$) halo stars (e.g. Gratton et al. 2000). These computed values are labelled as “Model” yields in Table 2.

For SNe Ia we use the yields of Iwamoto et al. (1999), specifically their case WDD1 (note however that for the elements considered in this paper a different choice of their SNe Ia model would not affect the results). For a consistent chemical evolution model, the metallicity of the pre-polluting SN Ia and AGB stars should be roughly the same as the external region ($[\text{Fe}/\text{H}]_{\text{ISM}}$), while the metallicity of the self-polluting SNe II match that of the inner region ($[\text{Fe}/\text{H}]_{\text{in}}$). Unfortunately, the set of yields of Iwamoto et al. (1999) are only available for solar metallicity and we are not aware of low-metallicity SNe Ia yields available in the literature.

In Table 3 we summarize the mean yields for intermediate-mass AGB stars, calculated by averaging the $Z = 0.0001$ values from Karakas & Lattanzio (2007) using a Salpeter (1955) IMF in the mass range 4–7 M_{\odot} (we will refer to this model as the “reference model”). As a comparison we also show the yield values obtained averaging similar datasets at the same metallicity published by Karakas & Lattanzio (2003) and Izzard et al. (2007), as well as the yields calculated by Fenner et al. (2004) for the specific case of AGB self-pollution in NGC 6752 at $[\text{Fe}/\text{H}] = -1.40$. In general, each set is in good agreement

Table 3. Mean SNe II, SNe Ia and intermediate-mass AGB yields in solar masses. SNe II yields refer to the model in Table 2. SNe Ia yields refer to the WDD1 model of Iwamoto et al. (1999). The mean AGB yields are averaged over the progenitor mass range 4–7 M_{\odot} using a Salpeter IMF for different authors: KA07=Karakas & Lattanzio (2007); FE04=Fenner et al. (2004); KA03=Karakas & Lattanzio (2003); IZ07=Izzard et al. (2007); all the yields are for $Z = 0.0001$ except for the case of Fenner et al. (2004) which is at $[\text{Fe}/\text{H}] = -1.40$. The yields of Fe and He are given in solar masses.

Polluter	Fe	He	C	N	O	Na	Mg	Al
Model (SNe II)	9.00e-2	6.00	1.59e-1	7.66e-3	1.82	1.60e-3	1.49e-1	3.23e-3
Model (SNe Ia)	6.72e-1	5.66e-3 ^a	5.42e-3	2.85e-4	8.82e-2	8.77e-5	7.69e-3	4.38e-4
AGB (KA07)	2.27e-5	1.45	6.21e-3	6.89e-2	1.44e-3	1.60e-3	2.17e-3	7.01e-5
AGB (FE04)	×	×	8.54e-3	5.76e-2	1.86e-3	5.95e-4	1.52e-3	6.13e-5
AGB (KA03)	×	×	×	×	×	7.79e-5	1.70e-3	1.04e-4
AGB (IZ07)	×	×	×	×	×	2.92e-5	2.15e-3	2.02e-4
Model (AGB)	2.27e-5	1.45	1.55e-3	6.89e-2	1.44e-3	4.00e-4	2.17e-3	3.50e-3

^a the value of He for SNe Ia is from Kobayashi et al. (2006).

although there are significant differences present for some elements (e.g., Na yields span ~ 2 orders of magnitude). A detailed study of how the production of the Ne, Na, Mg, and Al isotopes in AGB stars are effected by reaction rate uncertainties was carried out by Izzard et al. (2007). They concluded that the most uncertain yields are those of ^{26}Al and ^{23}Na , with variations of two orders of magnitude. The yields of ^{24}Mg and ^{27}Al have typical uncertainties of one order of magnitude. These uncertainties are comparable to those resulting from stellar modelling uncertainties, where differences of one order of magnitude or more can be found by varying the mass-loss rate or convective model Ventura & D’Antona (2005a,b) and Karakas et al. (2006b).

For this reason we also decided to use a set of *ad-hoc* intermediate-mass AGB yields that represent the different element production that we would require in order to reproduce the observational constraints in the framework of our model. This set of yields is presented in Table 3 as “Model”. These values are within the limits of the above-mentioned set of yields, and always within a factor of four of the values of the reference model (with the exception of Al see Section 5.3). In the following, the models using Karakas & Lattanzio (2007) (reference model) will be shown as solid lines, while the models using our proposed set of yields will be shown as dashed lines.

We would like to stress that the AGB yields we propose in Table 3 should not be taken as absolute values but as relative ratios between the different elements. This is because it is possible to re-scale the yields by changing the number of N_{AGB} stars needed to fit the observations. We use nitrogen as a reference element and re-scale the other elements accordingly. We choose nitrogen because it is better constrained than the other elements (e.g., Na, Al) since its production does not depend as strongly on reaction rate uncertainties. Note that the recent revision of the $^{14}\text{N}(p, \gamma)^{15}\text{O}$ reaction rate (Bemmerer et al. 2006), $\sim 60\%$ slower at temperatures below $100 \times 10^6 \text{K}$, would result in even more N production. Nitrogen yields are, however, effected by other modelling uncertainties such as convection, mass loss and the modelling of the third dredge-up (Marigo et al. 2003; Karakas et al. 2008). For example, an increase in the mass-loss rate would result in smaller N yields because of a shortened HBB phase (and also less Na, Mg and Al).

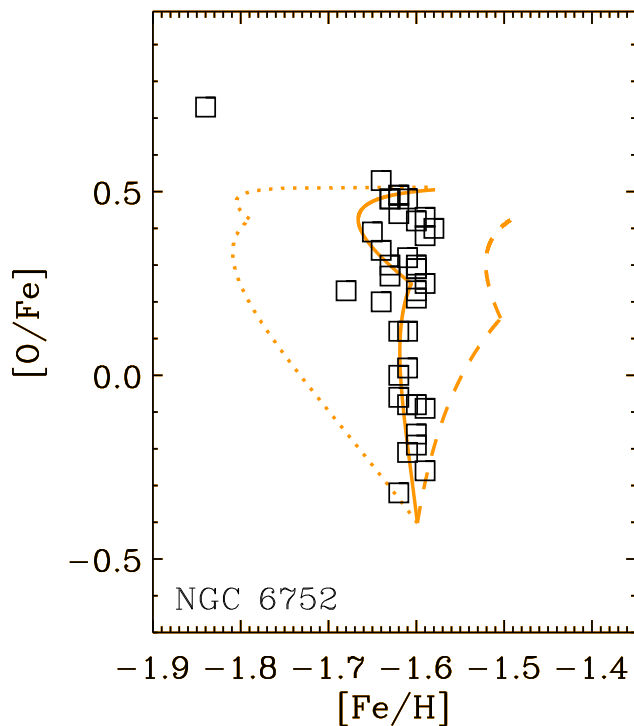


Figure 4. The predicted trend of $[\text{Fe}/\text{H}]$ versus $[\text{O}/\text{Fe}]$ for three models with different f_{exp} values compared with the observational dataset of Yong et al. (2005) for the case of NGC 6752. The initial values of f_{exp} are 1.0003 (dashed line), 1.0009 (solid line) and 1.0027 (dotted line) and are increased to 1.0012, 1.0035, and 1.015 after 750 SNe II have been exploded. The models are stopped after ~ 1600 SNe II have been exploded polluting the ISM. It is evident that changing the value of f_{exp} within a factor of three effects the $[\text{Fe}/\text{H}]$ ratio of the forming stars by only 0.1–0.2 dex.

5 RESULTS: THE CASE OF NGC 6752, M 13 AND NGC 2808

To test our framework in detail, we will focus on three well studied GCs: NGC 6752, M 13, and NGC 2808. All these GCs have an intermediate metallicity ranging from

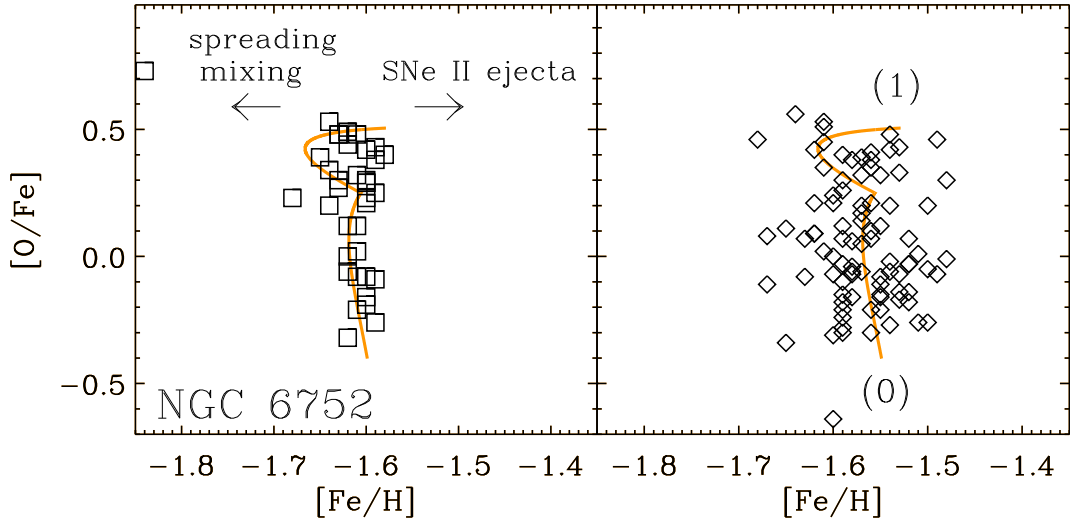


Figure 3. The predicted trend of $[\text{Fe}/\text{H}]$ versus $[\text{O}/\text{Fe}]$ compared with the observational dataset of Yong et al. (2005) (left panel) and Carretta et al. (2007) (right panel) for the case of NGC 6752. It is possible to maintain an invariant $[\text{Fe}/\text{H}]$ abundance owing to a tuning between the two opposing mechanisms: SNe II eject freshly synthesized Fe (and O), which is mixed with gas from the inner (inhomogeneous) volume along with material from the external ISM, which has a lower $[\text{Fe}/\text{H}]$ value.

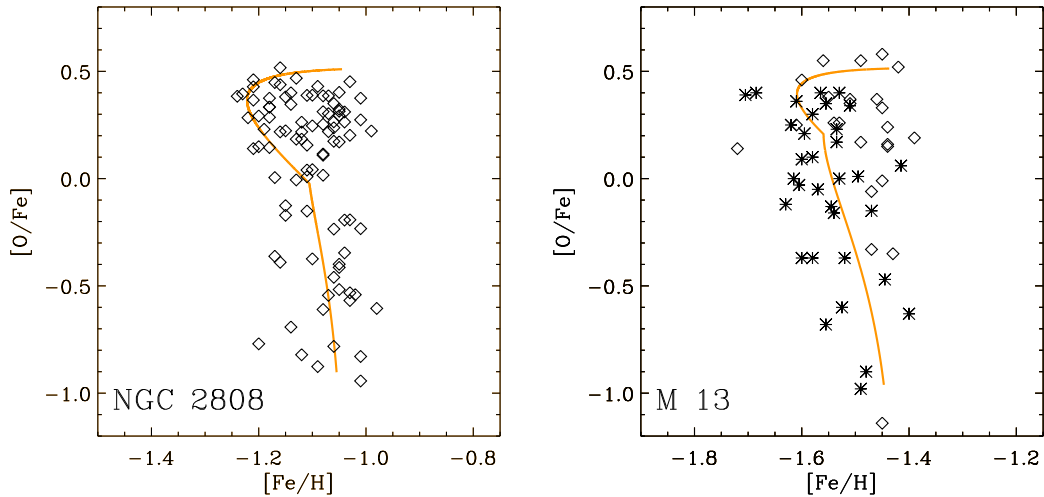


Figure 5. The predicted trend of $[\text{Fe}/\text{H}]$ versus $[\text{O}/\text{Fe}]$, for the case of NGC 2808 (left panel), compared with the observational dataset of Carretta et al. (2006). The case of M 13 (right panel) is plotted against the observational dataset of Sneden et al. (2004, asterisks) and Cohen & Meléndez (2005, diamonds).

$-1.60 \leq [\text{Fe}/\text{H}] \leq -1.10$ (e.g., Harris 1996). While NGC 6752 can be defined as a “normal” GC, NGC 2808 and M 13 show extreme values of the $[\text{O}/\text{Fe}]$ ratio (down to ~ -1.0) and are excellent cases to test our new proposed framework. In this section we show how different choices of the initial conditions in the pre-enrichment during the MW halo formation can lead to different chemical peculiarities in the forming GC.

5.1 $[\text{Fe}/\text{H}]$ and Metal content

Before going any further, it is important to follow the iron content of the forming stars in our model. As previ-

ously mentioned, the possibility of SNe II and SN Ia self-enrichment in GC have not been considered in the literature before, because they produce large amounts of Fe, whereas the $[\text{Fe}/\text{H}]$ content in most of the GCs appears to be constant.

The initial conditions of NGC 6752 are summarized in Table 1: the R_{in} of the inhomogeneous region polluted by the SN Ia is 36 pc and this volume is also polluted by 250 intermediate $4\text{--}7 M_{\odot}$ AGB stars. The mean iron content of the external region is $[\text{Fe}/\text{H}] = -2.55$, reflecting the early stage of the halo formation, while the effect of the SN Ia increases the value of $[\text{Fe}/\text{H}]$ up to -1.60 inside the inner region. In

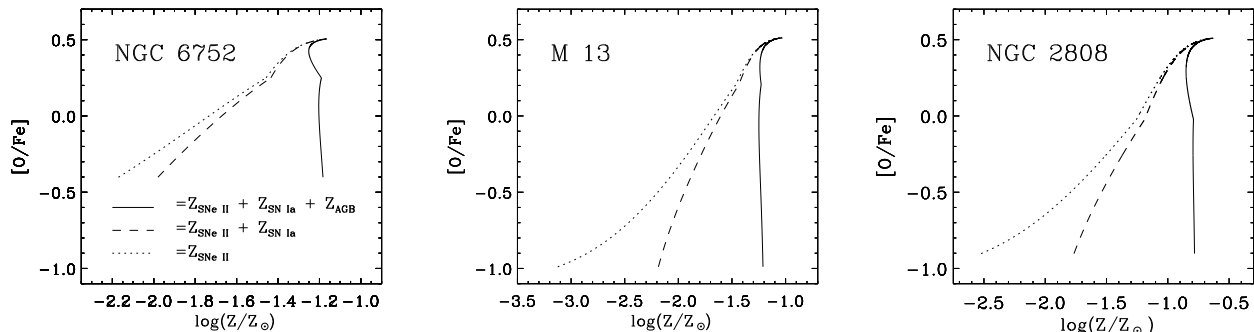


Figure 6. Evolution of the metallicity $\log(Z/Z_{\odot})$ versus $[O/Fe]$ in the inner region for the three reference models: NGC 6752 (left panel), M 13 (central panel), and NGC 2808 (right panel). The dotted line corresponds to the case where we ignored the contribution of the SN Ia+AGB pollution *only* to the total metallicity $\log(Z/Z_{\odot})$ (note that low initial $[O/Fe]$ value can be achieved only due to the localized contribution of the SN Ia), while dashed lines correspond to the model with no pollution from AGB stars. Note that the initial value of $\log(Z/Z_{\odot})$ (thus at low values of $[O/Fe]$) for the dotted line corresponds to the value of the metallicity for the external region. Most of the metals in the inner region are initially produced by AGB stars while at the end of the evolution only SNe II contribute to the metal content.

the same table, we also summarize the initial parameters for the cases of M 13 and NGC 2808.

For each GC, the initial conditions are constrained by the observed stellar values of $[Fe/H]$ and the peculiar values of $[O/Fe]_{\min}$ and $[Na/Fe]_{\max}$ (or alternatively the value of $[N/Fe]_{\max}$), as each of these values depends mainly on one polluter. Since most of the iron in the inner region is produced by SN Ia, the initial $[Fe/H]_{\text{in}}$ content of the forming stars is set by the value of R_{in} , while oxygen is produced mainly by SNe II and Na by intermediate-mass AGB stars (see Tables 2 and 3). We assume that a SN Ia always deposits the same amount of Fe ($0.74 M_{\odot}$), hence decreasing (increasing) the value of R_{in} has the effect of decreasing (increasing) the hydrogen content inside the inner region and increasing (decreasing) the $[Fe/H]$ content (this is evident in Table 1, where the value of $[Fe/H]_{\text{in}}$ increases for lower values of R_{in}). Once the $[Fe/H]$ content in the inner region is set, the overall $[Fe/H]_{\text{ISM}}$ value constrains the initial $[O/Fe]_{\min}$ of the model: this is because, according to a pure SNe II pollution model, the O content is proportional to the Fe content (and the Fe produced by SNe II can be ignored in the inner region). At this point, the observational value of $[Na/Fe]_{\max}$ is sufficient to constrain the number of intermediate-mass AGB stars needed to reproduce the Na-O anti-correlations.

For example NGC 6752 and M 13 have similar initial values of $[Fe/H]$, at $\simeq -1.60$ and $[Fe/H] \simeq -1.50$, respectively, that reflects comparable values of R_{in} . In contrast the “external” values of $[Fe/H]_{\text{ISM}}$ for each cluster differ by an order of magnitude (see Table 1 reflecting, as shown later, their different extreme values of $[O/Fe]$). In contrast, NGC 2808 shows an even higher value of $[Fe/H] \simeq -1.10$ because of its smaller value for $R_{\text{in}}=24$ pc, even if its $[Fe/H]_{\text{ISM}}$ is slightly lower than for the case of NGC 6752 (see Table 1).

In Fig. 3 we show the $[Fe/H]$ versus $[O/Fe]$ abundance evolution of the reference model for NGC 6752. Data from Yong et al. (2005) and Carretta et al. (2007) is included for comparison. To compare our model with the Carretta’s data, we apply an offset of 0.1 dex to our predicted value of $[Fe/H]$. This is to take into account a similar difference in the mean $[Fe/H]$ values between the two datasets. It is clear from the figure that the $[Fe/H]$ content remains relatively constant

during the whole evolution and it is consistent with the observational data. Likewise, the evolution of $[O/Fe]$ increases monotonically from its initial peculiar value $[O/Fe] \simeq -0.4$ to 0.5.

The $[Fe/H]$ abundance stays constant during the evolution because of the tuning between the two mechanisms changing the Fe content of the forming stars. While the newly exploding SNe II eject freshly synthesized Fe, increasing the $[Fe/H]$ content, their action also has the effect of expanding the inhomogeneous inner region, mixing the inner material with the external ISM (with a lower $[Fe/H]$ content). Both these two contrasting effects are controlled, in our model, by the parameter f_{exp} (i.e., the rate of expansion of R_{in} after each SN II explosion, see Eq. 1) which increases logarithmically with time. It is evident from Fig. 3 that, for this particular model, the effect of the expansion is, at the beginning, lowering the $[Fe/H]$ content, whereas at a later stage the SNe II pollution becomes increasingly dominant. The $[O/Fe]$ abundance of the forming stars starts increase monotonically during the evolution, as the Fe content is practically constant and SNe II ejects a large amount of O (a mean SN II produces $1.82 M_{\odot}$ of oxygen). Once the inhomogeneous region starts expanding, the O content of the forming stars reaches the asymptotic value of $[O/Fe]=0.5$, typical of pure SNe II pollution.

We use two different values of f_{exp} at two different stages, as this gives a better fit to the data. For example, for NGC 6752, the initial value of 1.0003 is increased to 1.001 after $\sim 10^3$ SNe II have exploded. The effect on the model of this variation can be seen in Fig. 3 as a small “hook” at $[O/Fe] \sim 0.25$. Even if it were possible to better tune the model (by using another expansion law or simply by finding the best parameter combination to maintain $[Fe/H]$ perfectly constant during the evolution), we are confident that such a fine tuning is not necessary and would not significantly change our conclusions. Indeed, given all the other model uncertainties we think it is unnecessary to attempt to fine tune the expansion caused by the SN II explosions. However, to check the robustness of our conclusions to the assumed expansion value, we show in Fig. 3 the predicted trend of $[Fe/H]$ vs. $[O/Fe]$ for three different values of f_{exp} (roughly

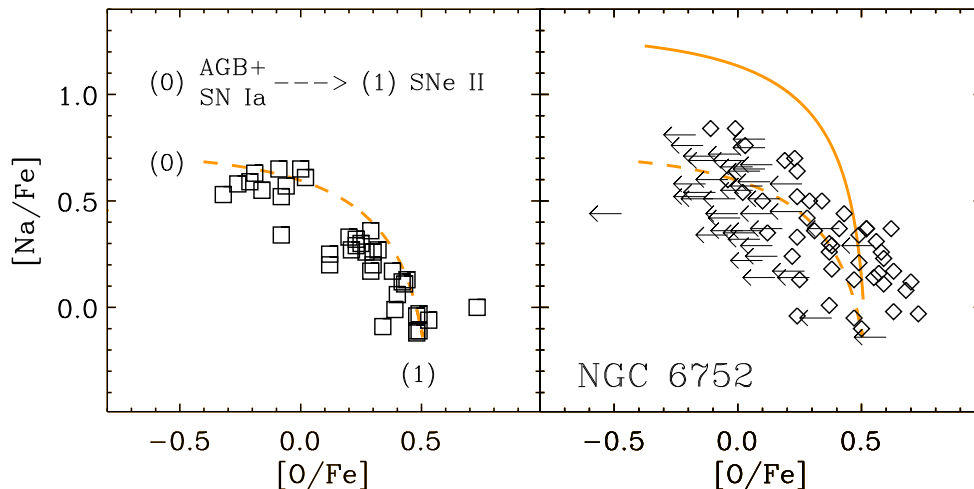


Figure 7. The predicted evolution of the $[\text{Na}/\text{Fe}]$ versus $[\text{O}/\text{Fe}]$ abundance for NGC 6752, plotted against the observational datasets of Yong et al. (2005) (left panel) and Carretta et al. (2007) (right panel, arrows refer to upper limit values; see the original paper for details). In our framework the AGB+SN Ia pollution is due to pre-existing halo stars while only SNe II self-pollute the GC. The solid line in the right panel refers to the reference model using the yields of Karakas & Lattanzio (2007) while the dashed lines refer to a model with Na production lowered by a factor of four compared with the reference model (see Table 3).

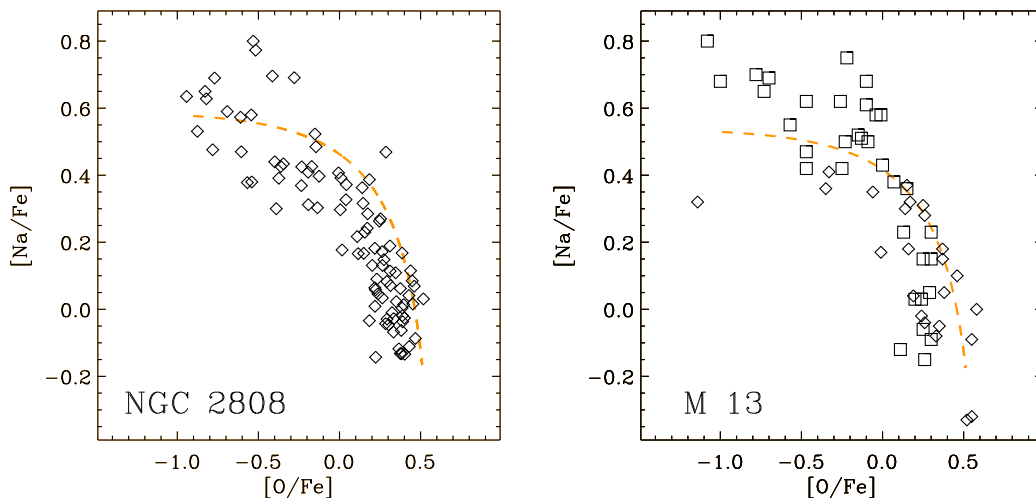


Figure 8. (Left panel) the predicted evolution of the $[\text{Na}/\text{Fe}]$ versus $[\text{O}/\text{Fe}]$ abundance for NGC 2808 against the observational data from Carretta et al. (2006). (right panel) the same trend for the case of M 13 plotted against the observational data from Sneden et al. (2004) (squares) and Cohen & Meléndez (2005) (diamonds).

spanning a factor of 10 in dynamic range). It can be seen that changing f_{exp} by a factor of three affects the $[\text{Fe}/\text{H}]$ ratio of the forming stars by only 0.1-0.2 dex.

In Fig. 5 we compare the results from our model with NGC 2808 and M 13. These GCs were chosen on the basis of their peculiar O depletion with values of $[\text{O}/\text{Fe}]$ as low as -1.0 . These low values are very difficult to obtain with only primordial self-enrichment, which may explain the oxygen depletion down to a minimum value $[\text{O}/\text{Fe}] \sim -0.5$ but no lower. Extra mixing may also contribute to the depletion of oxygen but only for stars near the tip of the first giant branch. D’Antona & Ventura (2007) invoke a combination of the two to explain the case of M 13, while in the model

of Bekki et al. (2007) such extreme values are achieved by assuming that no third dredge-up occurs in intermediate-mass AGB stars.

We are able to reproduce the low values of $[\text{O}/\text{Fe}]$ without any particular assumption (see Fig. 5). Indeed, such low $[\text{O}/\text{Fe}]$ values arise naturally if the inhomogeneous region – polluted by the initial SN Ia – is smaller in the case of NGC 2808 and M13 than NGC 6752 (see Table 1). In the case of M 13, the extreme low values of $[\text{O}/\text{Fe}]$ of -1.0 requires a slightly smaller R_{in} as well as less oxygen from the SNe II that pre-polluted the halo. To fit the properties of M 13, the metallicity of the original ISM gas at the time of GC formation needs to be very low, with

a typical $[\text{Fe}/\text{H}]$ abundance an order of magnitude lower ($[\text{Fe}/\text{H}]_{\text{ISM}} = -3.50$) than for NGC 2808 or NGC 6752. This is despite the final $[\text{Fe}/\text{H}]$ of M 13 is similar to NGC 6752. The lower initial of $[\text{Fe}/\text{H}]_{\text{ISM}}$ for M 13 than for NGC 6752 could indicate that this GC formed at an earlier epoch and that it is older than the other two GCs. Photometric ages of M M13 compared to NGC 6752 suggest that M 13 is older (Rakos & Schombert 2005), but these age determinations are highly uncertain and should be treated as tentative.

In Fig. 6 we show the evolution of the logarithm of the metallicity ($\log(Z/Z_{\odot})$) versus the $[\text{O}/\text{Fe}]$ abundance inside the inner region for the above models (solid lines). As in the case of the $[\text{Fe}/\text{H}]$ abundance, the total metallicity remains approximately constant during the evolution. The dashed lines represent the same evolution without taking into account the contribution of metals by intermediate-mass AGB stars to the total metallicity fraction. The dotted lines represent the case in which the contribution of SN Ia and AGB to the total metallicity are ignored (that is, only SNe II contribute to the global metallicity). Most of the initial metals (e.g., C, N) inside the inner region are due to localized AGB pollution, while the SN Ia contribution is minimal. Indeed, even if a SNe Ia ejects large amounts of Fe ($0.74 M_{\odot}$) they eject only $1.4 M_{\odot}$ of total metals. Most of the “metal” are instead produced by AGB stars (an intermediate-mass AGB star produces a mean value $\sim 0.08 M_{\odot}$ of metals, most of which is N; see Table 3). At the end of the evolution, most of the metals are produced by SNe II, where all lines converge to the same value in Fig. 6. This is also demonstrated by the asymptotic value of $[\text{O}/\text{Fe}] = 0.5$ typical of pure SNe II pollution. Since the metallicity of the stars is roughly constant during the evolution this is also the metallicity of the forming stars.

We do not have a parameter that sets the fraction of SNe II that pollute the forming stars. Instead we calculate that assuming the initial mass of the GC is the same as it is today (Pryor & Meylan 1993), and assuming a constant density and metallicity for the gas in the inner region, the fraction of SNe II ejecta that directly enriches the inner 30 (50) pc (i.e., where the GC star should be forming) turns out to be very low, of the order of 0.5-1% (3-6%), depending on the details of the model. Indeed, most of the metals produced by the SNe II are expelled beyond this limit of ~ 50 pc.

5.2 The O-Na anti-correlation

Intermediate-mass AGB stars do not produce Fe and O (Karakas & Lattanzio 2007), hence they have a negligible contribution to the evolution of these elements. AGB stars do, however, produce a considerable amounts of Na.

In Fig. 7 we show the evolution of $[\text{O}/\text{Fe}]$ versus $[\text{Na}/\text{Fe}]$ abundances predicted by our model, together with the observational data from Yong et al. (2005) and Carretta et al. (2007, ; upper limits are shown as arrows) for the case of NGC 6752. As already mentioned, the first stars to form in our model are $[\text{Na}/\text{Fe}]$ -rich (due to the Na-rich AGB pollution) and $[\text{O}/\text{Fe}]$ -depleted (due to the localized iron-rich SN Ia ejecta). The effect of the SN Ia is to mitigate the increase of the $[\text{Na}/\text{Fe}]$ abundance that would otherwise reach much higher values. For example, in Fenner et al. (2004) the $[\text{Na}/\text{Fe}]$ abundance increased to $[\text{Na}/\text{Fe}] \simeq 1.7$. Once the first SNe II starts to pollute the ISM and the

Table 4. Isotopic ratios for the mean yields of SNe II, SNe Ia, and AGB models. Notations are as in Tables 2 and 3.

	$^{25}\text{Mg}/^{24}\text{Mg}$	$^{26}\text{Mg}/^{24}\text{Mg}$	$^{12}\text{C}/^{13}\text{C}$
SNe II (W&W)	7.2×10^{-3}	6.3×10^{-3}	10^4
SNe II (KOB)	9.9×10^{-3}	8.9×10^{-3}	10^3
SNe II (C&L)	2.8×10^{-3}	5.0×10^{-3}	5×10^4
Model (SNe II)	10^{-2}	10^{-2}	10^4
AGB (KA07)	6.5	20.7	6.0

inhomogeneous region expands, the chemical properties of the forming stars evolve toward “normal” $[\text{Na}/\text{Fe}]$ -poor and $[\text{O}/\text{Fe}]$ -rich. In the figure we show two different predictions using 1) our reference model yields, and 2) the same yields but with the Na yields from Karakas & Lattanzio (2007) reduced by a factor of four. While the reference model shows a clear O-Na anti-correlation, qualitatively in agreement with the observations, it overestimates the initial value of $[\text{Na}/\text{Fe}]$ by ~ 0.4 - 0.6 dex. In comparison, the model with the reduced Na yields reproduces better the observed anti-correlation. Note that the reduced value ($\langle \text{Na} \rangle = 4.0 \times 10^{-4} M_{\odot}$) is in better agreement with the Na production reported by Fenner et al. (2004) ($\langle \text{Na} \rangle = 5.9 \times 10^{-4} M_{\odot} M_{\odot}$), and by Karakas & Lattanzio (2007) for more metal-rich AGB stars ($\langle \text{Na} \rangle = 7.7 \times 10^{-4} M_{\odot}$ for $Z = 0.004$). The reduced Na yields are also well within model uncertainties (see Table 3). It is also possible to obtain a very good match to the absolute values of $[\text{Na}/\text{Fe}]$ by simply reducing (by same factor of 4) the amount of AGB pollution compared to the reference model (see Table 1), because the number of AGB stars has little effect on O and Fe (see Table 3). However, as discussed in Sec. 4, we use AGB nitrogen production as a reference (see § 5.5). Thus, in the following we will always assume a mean value of $\langle \text{Na} \rangle = 4.0 \times 10^{-4} M_{\odot}$ from intermediate-mass AGB stars.

The $[\text{O}/\text{Fe}]$ versus $[\text{Na}/\text{Fe}]$ abundance evolution for the models tailored for NGC 2808 and M 13 are shown in Fig. 8, along with their respective observational datasets. The O-Na anti-correlation is well reproduced for these two GCs, including the extremely low values of $[\text{O}/\text{Fe}]$.

5.3 The Mg-Al anti-correlation

In the left panel of Fig. 9 we compare the predictions of our reference model (solid line) for NGC 6752 with the observed Al-Mg anti-correlation found by Yong et al. (2005). This dataset shows anti-correlations in stars that are both brighter and fainter than the first giant branch bump, strongly suggesting that the peculiarities should be present in the gas from which the stars formed, and not caused by internal stellar evolution. It is apparent that there is a spread of ~ 1.3 dex in Al relative to Fe but only a modest spread of ~ 0.3 dex in Mg relative to Fe (the corresponding $[\text{O}/\text{Fe}]$ spread discussed in Section 5.2 is ~ 1.0 dex).

In our framework, the first stars to form have enhanced Al ($[\text{Al}/\text{Fe}] \simeq 1.4$) and depleted Mg ($[\text{Mg}/\text{Fe}] \simeq 0.2$), while subsequent generations evolve toward $[\text{Al}/\text{Fe}] \simeq 0.0$ and $[\text{Mg}/\text{Fe}] \simeq 0.5$. It is apparent that our reference model (Fig. 9) can only account for the Mg variation and fails to

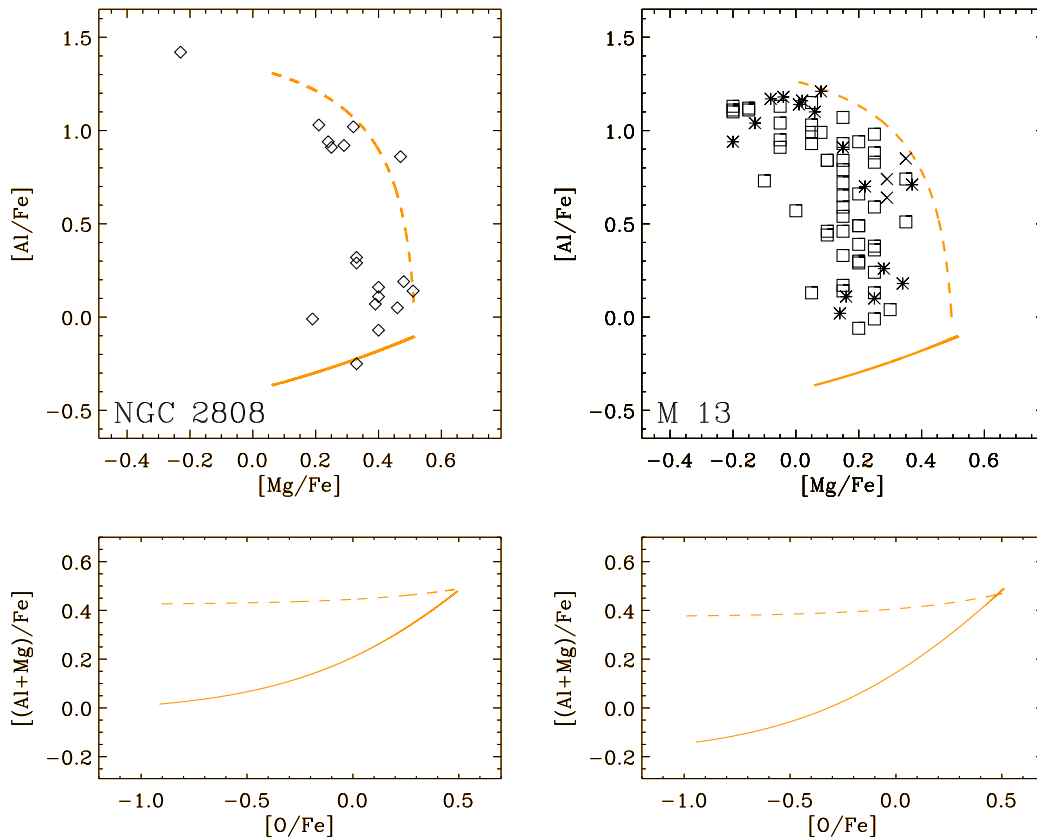


Figure 10. Upper panels: the evolution of the $[\text{Al}/\text{Fe}]$ versus $[\text{Mg}/\text{Fe}]$ abundance for NGC 2808 (left panel) and M 13 (right panel). As in Fig. 9, the solid lines refer to the model using yields from Karakas & Lattanzio (2007), whereas the dashed lines refer to the model with increased Al from AGB stars. The evolution is plotted against the observational datasets of Carretta et al. (2006) for the case of NGC 2808 (left panel) and Sneden et al. (2004, asterisks), Johnson et al. (2005, squares) and Cohen & Meléndez (2005, crosses) for the case of M 13. Regarding M 13, we point out that there is an offset of 0.2 dex for the Mg abundance between our model and the observational dataset. Bottom panels: the predicted $[(\text{Al}+\text{Mg})/\text{Fe}]$ versus $[\text{O}/\text{Fe}]$ abundances; line styles are as above.

reproduce the ~ 1.5 dex spread in Al. The small amount of Al produced in the models of Karakas & Lattanzio (2007) is not enough to countervail the large amount of Fe deposited by the single SN Ia: the net results is that the $[\text{Al}/\text{Fe}]$ ratio actually decreases in our model. Note that even in the case of pure AGB pollution (Fenner et al. 2004), the maximum $[\text{Al}/\text{Fe}]$ value is underestimated by a factor of ~ 0.7 dex. If we assume that low-metallicity AGB stars produce a mean value of $\text{Al} \sim 3.5 \times 10^{-3} M_{\odot}$ (instead of the literature values of $\sim 10^{-4} M_{\odot}$) shown in Table 3, the Al-Mg anti-correlation is remarkably well reproduced.

In the upper panels of Fig. 10, we plot the $[\text{Mg}/\text{Fe}]$ versus $[\text{Al}/\text{Fe}]$ evolution of our reference models for M 13 (right panel) and NGC 2808 (left panel) against the corresponding observational datasets (Sneden et al. 2004; Johnson et al. 2005; Cohen & Meléndez 2005; Carretta et al. 2006). Again the reference models are not able to reproduce the Al enhancement, while models with a factor of ~ 50 more Al production from intermediate-mass AGB stars are able to reproduce the anti-correlation perfectly. The dotted line in the right panel represents the same dashed line but offset by 0.2 dex in $[\text{Mg}/\text{Fe}]$. At low $[\text{Al}/\text{Fe}]$ values there is a difference of ~ 0.2 dex between the $[\text{Mg}/\text{Fe}]$ values of the two GCs.

At this point, it is worth asking if our proposed Al yield ($\sim 3.5 \times 10^{-3} M_{\odot}$) from intermediate-mass AGB stars is consistent with the uncertainties present in the theoretical models, as well as with other available observations in other systems. To test this latter point, we ran a test chemical evolution model of the Milky Way using GEtool (Fenner et al. 2002) with the same enhancement in Al AGB yields that is required for the GC model. The result is only a small difference (within $\sim 0.2 - 0.3$ dex and only for $[\text{Fe}/\text{H}] \geq -1.6$) compared with the canonical MW model.

The yields of ^{27}Al are affected by variations in the nuclear reaction rates, as well as the treatment of mass loss and convection. For example both, the $^{26}\text{Mg}(p,\gamma)^{27}\text{Al}$ and $^{26}\text{Al}(p,\gamma)^{27}\text{Si}$ reactions play an important role in determining the final ^{27}Al abundance in a given AGB model. Izzard et al. (2007) concluded that the yields of ^{26}Al and ^{27}Al can vary by up to ~ 2 orders of magnitude, depending on the mass, metallicity and choice of Mg-Al reaction rates. The yields of Al decrease with increasing mass loss, because more mass is lost before significant Al can be synthesized from Mg via the HBB. The yields of nitrogen and Al (but also C, Na and Mg) depend also on the third dredge-up (Ventura & D’Antona 2005a,b; Karakas et al. 2006b). While there is uncertainty

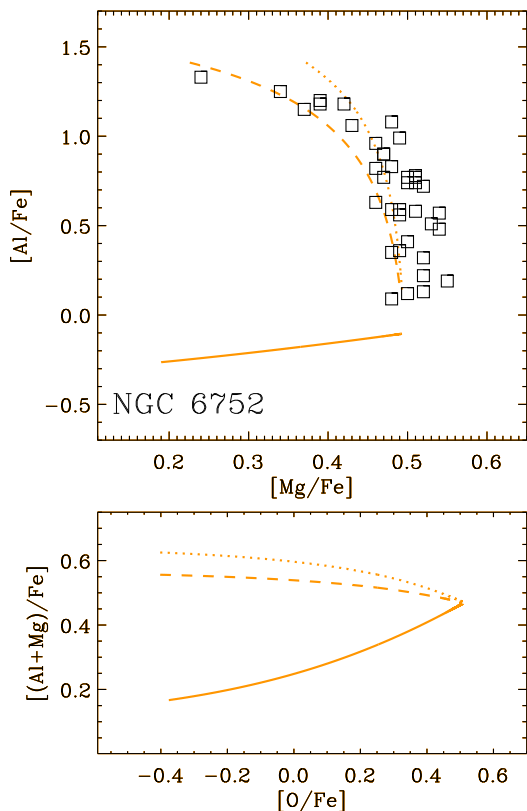


Figure 9. Upper panel: the predicted evolution of the $[\text{Al}/\text{Fe}]$ versus $[\text{Mg}/\text{Fe}]$ abundance for NGC 6752. Also shown is the observational dataset of Yong et al. (2005). The solid line refers to the model with canonical Al yields from Karakas & Lattanzio (2007) while the dashed line refers to our assumed mean Al production ($\text{Al}=3.5 \times 10^3 M_{\odot}$) from AGB stars that is required to reproduce the observations. The dotted line refers to the previous model but with a 50% enhancement of the ^{25}Mg and ^{26}Mg yields from AGB stars (see Section 5.4 for more details of this model). Bottom panel: the predicted evolution of the sum $[(\text{Al}+\text{Mg})/\text{Fe}]$ versus $[\text{O}/\text{Fe}]$ for the three models described above; line styles are the same.

over the amount of dredge-up in intermediate-mass AGB stars, observations suggest that it should be fairly efficient (Wood et al. 1983; García-Hernández et al. 2006). Moreover, hot-bottom burning is the major production site for Al (as well as for Na and Mg). In Fig. 9 we show that increasing the AGB yields of Mg by 50% (particularly ^{25}Mg and ^{26}Mg , see next subsection) does not have a significant effect on the ability of the model to reproduce the Mg-Al anti-correlation observed in NGC 6752. It is not clear, however, if the model uncertainties would allow for an increase in the Al abundance by a factor of 50 and further study of this problem is required.

Using data for 18 stars, Carretta et al. (2007) noted that the sum of Mg+Al is approximately constant in NGC 2808 for stars in all evolutionary phases (that is, constant over the whole magnitude range). The conclusion to be drawn from this observation is that there has been a reshuffling of Mg into Al in these stars. The bottom panels of Fig. 9 and Fig. 10 show the sum of Mg+Al of our mod-

els plotted against the $[\text{O}/\text{Fe}]$ abundance. If we assume the above mentioned Al enhancement in AGB yields, the sum Al+Mg appears to be surprisingly constant (in the reference model this sum is only constant within a factor of two). Increasing the yields of Mg by 50% does not change this result, and the sum of Mg+Al is constant to within 0.1 dex (dotted line).

5.4 The Mg isotope ratios

A further important test for our model is determining how well it can reproduce the Mg isotopic ratios observed in GC stars (e.g. for NGC 6752 Yong et al. 2003). The Mg production from AGB stars is mainly in the form of the neutron-rich magnesium isotopes, ^{25}Mg and ^{26}Mg , which are produced in the He-burning shell (e.g. Karakas & Lattanzio 2003). In Table 4 we summarize the mean $^{25}\text{Mg}/^{24}\text{Mg}$ and $^{26}\text{Mg}/^{24}\text{Mg}$ ratios for the intermediate-mass AGB yields of Karakas & Lattanzio (2007), as well as the same ratios for different SNe II models computed by different authors. It is apparent that the ratios $^{25}\text{Mg}/^{24}\text{Mg}$ and $^{26}\text{Mg}/^{24}\text{Mg}$ are much higher in the case of AGB pollution compared to SNe II, where SNe II preferentially produce ^{24}Mg at low metallicities. In the following we will adopt a constant value of 0.01 for both $^{25}\text{Mg}/^{24}\text{Mg}$ and $^{26}\text{Mg}/^{24}\text{Mg}$ to reflect SNe II (see Table 4; adopting values from different authors does not significantly change the results).

In Fig. 11 we show the observed Mg isotopic ratios for NGC 6752 from Yong et al. (2003), plotted against the $[\text{O}/\text{Fe}]$, $[\text{Na}/\text{Fe}]$, $[\text{Mg}/\text{Fe}]$, and $[\text{Al}/\text{Fe}]$. In this figure we include the predictions from our reference model (solid lines). The agreement is satisfactory, except in the case of Al (solid line) which, as already discussed, can be accommodated by assuming a larger Al production from AGB stars (dashed line). Both the $^{25}\text{Mg}/^{24}\text{Mg}$ and $^{26}\text{Mg}/^{24}\text{Mg}$ ratios decrease as the GC stars evolve from the AGB-SN Ia peculiar pollution ($^{25}\text{Mg}/^{24}\text{Mg} \sim 0.5$ and $^{26}\text{Mg}/^{24}\text{Mg} \sim 0.15$), to predominantly self pollution by SNe II ($^{25}\text{Mg}/^{24}\text{Mg} \sim 0.01$ and $^{26}\text{Mg}/^{24}\text{Mg} \sim 0.01$).

All GC chemical evolution models so far have failed to reproduce the Mg isotopic ratios observed in NGC 6752 (e.g. Fenner et al. 2004; Ventura & D’Antona 2005c). One of the strongest conclusions from Fenner et al. (2004) was that it is not possible to reproduce the Mg-Al anti-correlation and the Mg isotopic ratios with a classical AGB self pollution scenario. This is because AGB stars *produce* Mg instead of destroying it, and thus Mg and Al are correlated. In our model the $[\text{Mg}/\text{Fe}]$ depletion is mainly caused by the effect of the SN Ia, hence the production of Mg from AGB stars is not significant. The Mg production instead helps to explain why strong $[\text{O}/\text{Fe}]$ depletions (of up to -0.5) are not accompanied by a similarly low $[\text{Mg}/\text{Fe}]$ abundances. Even an increase of 50% in the ^{25}Mg and ^{26}Mg yields from AGB models does not effect our conclusions, and instead meliorates the Mg isotopic ratios when plotted against $[\text{Mg}/\text{Fe}]$ (see Fig. 11).

Note that varying the Mg ratios in the SNe II yields from $^{25}\text{Mg}/^{24}\text{Mg}$ and $^{26}\text{Mg}/^{24}\text{Mg} \sim 0.01$ to 0.1 would help to fit the observational data. In Fig. 12 we show the Mg isotopes ratios versus $[\text{Na}/\text{Fe}]$ from Yong et al. (2006a) in the case of M 13 together with the predictions from our model and, again, the observations are matched fairly well.

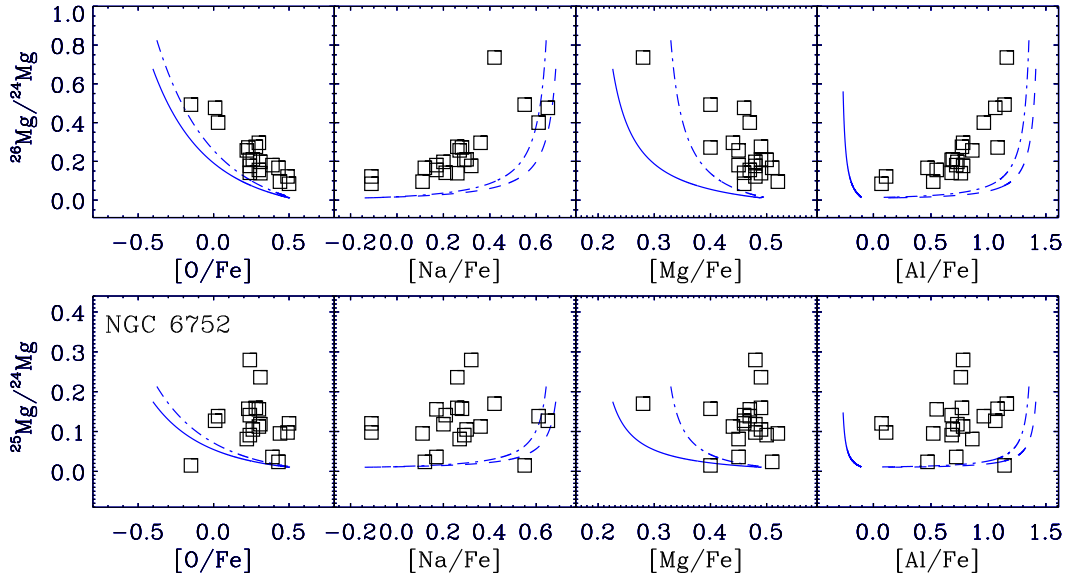


Figure 11. Predicted evolution of the Mg isotopic ratios versus $[O/Fe]$, $[Na/Fe]$, $[Mg/Fe]$, and $[Al/Fe]$ for our model (dashed lines). The dashed lines refers to our assumed “Model” (see Table 3), while the dotted lines represent the evolution in the case of the ^{25}Mg and ^{26}Mg AGB yields increased by 50%. (see Table 4).

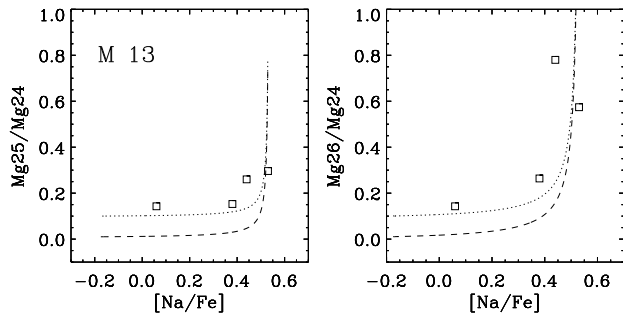


Figure 12. Predicted evolution of Mg isotopic ratios versus $[Na/Fe]$ for our reference model (solid lines) compared with the observational data from Yong et al. (2006a). The dashed lines correspond to the model with $^{25}\text{Mg}/^{24}\text{Mg}=0.1$ and $^{26}\text{Mg}/^{24}\text{Mg}=0.1$ from SNe II (instead of 0.01; see Table 4).

Assuming $^{25}\text{Mg}/^{24}\text{Mg}=0.1$ and $^{26}\text{Mg}/^{24}\text{Mg}=0.1$ for the SNe II yields does an even better job at reproducing the observations.

5.5 The C-N anti-correlation

In Fig. 13 we illustrate the evolution of $[C/Fe]$ versus $[N/Fe]$ of our reference model for NGC 6752, together with observational data by Carretta et al. (2005) for 9 dwarfs (filled diamonds), 9 sub-giants stars (open diamonds), along with 2 giants stars (open triangles) observed by Smith & Norris (1993). Comparison with stars near the main sequence is preferred, because variations due to the first dredge-up and deep mixing can affect the abundances of evolved stars. However, it is very difficult to obtain high-quality spectra of main-sequence stars owing to their low brightness. In the following we will not discuss

the effect of stellar evolution on the changes to the surface abundances of C and N (instead we refer the interested reader to Smith & Tout 1992; Charbonnel 1994, 1995; Denissenkov & Tout 2000; Weiss et al. 2000; Gratton et al. 2004, and references therein).

While the more evolved stars (open symbols) show a clear C-N anti-correlation, similar to that observed in other GCs (see also Fig. 14 for M 13), the inclusion of the dwarf stars makes it difficult to distinguish a clear evolutionary pattern. Carretta et al. (2005) pointed out that the spectra for these turn-off stars did not have enough quality to allow for an accurate determination of the carbon abundances; the same also applies to the $^{12}\text{C}/^{13}\text{C}$ ratios (see § 5.7). Typical errors for the $[C/Fe]$ abundances are of the order of ~ 0.2 dex with the exception of the dwarf stars that show larger uncertainties.

A quick examination of Table 3 shows that nitrogen is the element produced in the largest proportions by intermediate-mass AGB stars. Thus, it is not surprising that the first stars forming in the inner region initially polluted by AGB stars show very high values of $[N/Fe]$ (~ 1.5) despite the action of the SN Ia. For comparison, in Fenner et al. (2004), stars polluted with AGB ejecta show $[N/Fe]$ values as high as ~ 2.0). Carbon is also produced in intermediate-mass AGB stars, although not to the same level as N, hence the $[C/Fe]$ ratios remains low. A glance at Fig. 13 shows that while a large variation of $[N/Fe]$ is achieved in our model in accordance with observations, the ratio of $[C/Fe]$ remains almost constant. While $[C/Fe] \sim 0.0$ at high values of $[N/Fe]$ is consistent with the observed $[C/Fe]$ abundances inferred from dwarf stars, assuming a factor of 4 less carbon is produced by AGB stars does a much better job of reproducing the C-N anti-correlation observed in sub-giant stars. (see Fig. 13 and Table 3).

The C-N anti-correlation is also seen for stars on the

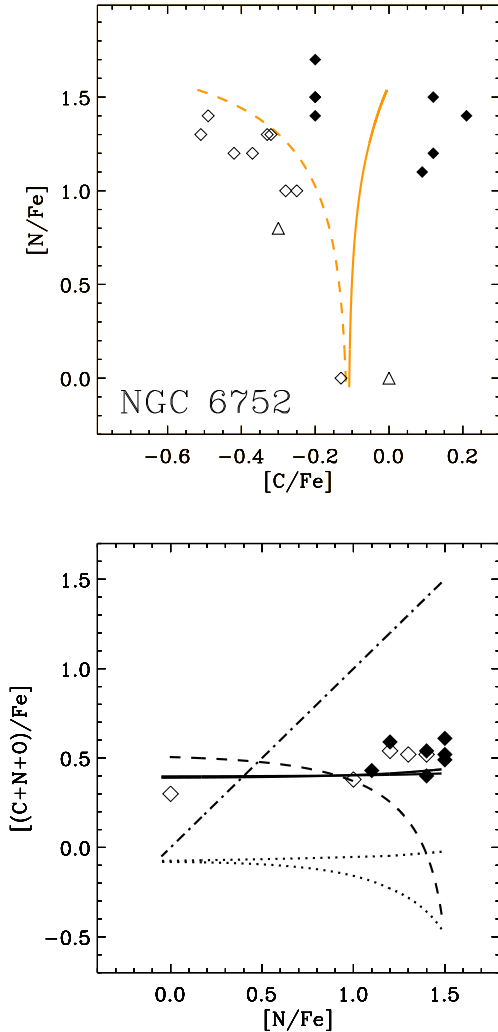


Figure 13. Upper Panel: evolution of $[C/Fe]$ versus $[N/Fe]$ for the reference model (solid line) for NGC 6752, plotted against observational data of two AGB stars by Smith & Norris (1993) (triangle), and 9 sub-giants stars (open diamonds) and 7 dwarf stars (filled diamonds) by Carretta et al. (2005) (squares). The dashed line represents the model with AGB C yields decreased by a factor of 4. Lower panel: evolution of the sum of $[(C+N+O)/Fe]$ (solid lines) for the reference model (thick lines) and well as for the model with reduced C (thin lines) plotted against the observational dataset of Carretta et al. (2005); the symbols are the same as in the upper panel. The evolution of each single element is also shown: C (dotted lines), N (dot dashed line), and O (dashed line).

main sequence turn off of M 13 (Briley et al. 2004b) (see Fig. 14), whereas we are not aware of a similar dataset for NGC 2808 (although the C-N evolution of this GC is similar to M 13 for more evolved stars). We refer to Briley et al. (2004b) for a discussion of the uncertainties affecting the abundances; these can be large (up to 0.5 dex, see their Fig. 5) owing to the faintness of the observed stars. Again the two models show quite similar results, with $[C/Fe]$ remaining approximately constant in the reference model, and the model that assumes C is under produced by a factor of 4 doing the best job of reproducing the C-N anti-correlation.

To test the possible contribution of low-metallicity fast rotators or mass loss in metal-poor massive stars (Meynet & Maeder 2002b,a) we qualitatively increase the nitrogen mean yield for SNe II, from our reference value of $[N/Fe]=-0.90$ to values of $[N/Fe]=-0.30$ and 0.0 . This increase only slightly changes the results, by increasing the minimum value of $[N/Fe] \simeq -0.4$ in Fig. 14 by a factor of 0.20-0.40 dex.

5.6 The sum of C+N+O

One of the most important observational constraints that any GC chemical evolution model needs to fulfill is the constancy of the sum C+N+O (e.g. Ivans et al. 1999; Carretta et al. 2005). Self pollution scenarios using AGB models calculated using the mixing-length theory (MLT) of convection (Fenner et al. 2004; Karakas et al. 2006a) predict that stars forming from different generations of AGB ejecta show large increases in the CNO sum. This is in contrast to AGB models computed using the “full spectrum of turbulence” convective model (Ventura & D’Antona 2005b) that manage to keep the sum of CNO constant within a factor of two. This is because the Ventura & D’Antona (2005b) show little third dredge-up (which increases C and hence N) and more efficient HBB (which converts C and O to N). Hence, MLT models create C and N rich AGB ejecta at almost constant O (see Fig. 4 in Fenner et al. 2004). FST models result in moderately O-depleted AGB ejecta that is only moderately enriched in N Ventura & D’Antona (2005b).

In the bottom panel of Fig. 13 we show the C+N+O sum (solid line) of our model for NGC 6752, together with $[C/Fe]$ (dotted lines), $[N/Fe]$ (dot-dashed line) and $[O/Fe]$ (dashed line) plotted against $[N/Fe]$. In the same figure we also include the observational data from Carretta et al. (2005) for 5 sub-giants and 7 dwarf stars from the same GC. It is quite remarkable that our model predicts a practically constant CNO sum and is a satisfactory fit to the observations. It is apparent that while the $[C/Fe]$ abundance remains approximately constant, a large variation of $[N/Fe]$ comes with a similarly large variation in $[O/Fe]$. The N deposited by AGB stars is counteracted by the O production in SNe II when the inner region expands and mixes (lowering the $[N/Fe]$ value). In principle, in our model, there is no reason for this to happen because the mechanisms controlling the Fe abundance and the CNO sum are different (i.e., SNe II, SN Ia, and AGB). For example, more AGB pollution (or no AGB pollution at all) would increase (decrease) the initial CNO sum and the condition $C+N+O=\text{constant}$ would not be fulfilled. However, in the three particular GC considered here, once the free parameters are fixed to reproduce the observed anti-correlations, a constant C+N+O naturally arises.

The thin solid lines and dotted lines in the lower panels of Fig. 13 and Fig. 14 refer to the case in which the C production from AGB stars is lowered by a factor of 4 to better fit the C-N anti-correlation. In this case the sum of C+N+O also remains quite constant, in agreement with the observations. The fact that a variation of 0.4 dex of the $[C/Fe]$ abundance only slightly changes the CNO sum is understandable if we consider that O and N are a factor of ~ 8 more abundant than C at low values of $[N/Fe]$ and high values of $[N/Fe]$, respectively.

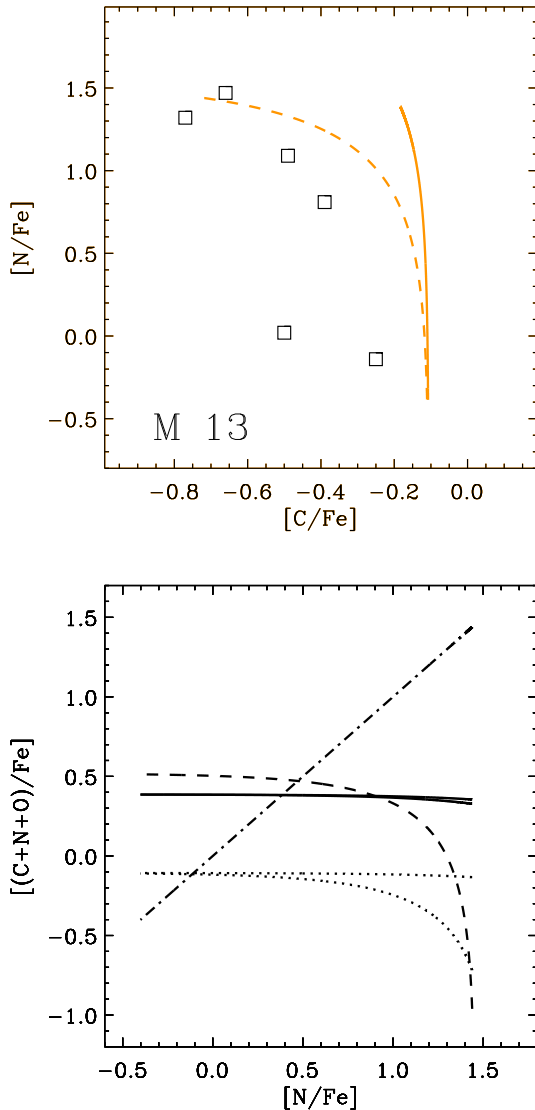


Figure 14. M 13 Upper Panel: evolution of $[C/Fe]$ versus $[N/Fe]$ for the reference model (solid line) plotted against the observational data of Briley et al. (2004a). The dashed line corresponds to the model where we decrease the C yields from AGB stars by a factor of 4. Lower panel: the evolution of the sum of $[(C+N+O)/Fe]$ (solid lines) for the reference model (thick lines) as well as for the model with reduced C (thin lines). The evolution of each single element is also shown: C (dotted lines), N (dot dashed line) and O (dashed line). The corresponding two diagrams for the case of NGC 2808 are almost identical to the results for M 13 and not shown.

5.7 The carbon isotope ratio

In Fig. 15 we show the evolution of the $^{12}C/^{13}C$ ratio versus $[Na/Fe]$ from our model plotted against observational data from Carretta et al. (2005) for sub-giant stars in NGC 6752. Owing to the poor quality of the spectra, these authors were not able to derive the carbon isotopic ratio for dwarf stars. Our model over-predicts the $^{12}C/^{13}C$ ratio at any value of $[Na/Fe]$ and by up to a factor of 1.5 dex. Chiappini et al. (2008) and Hughes et al. (2008) note that a model without

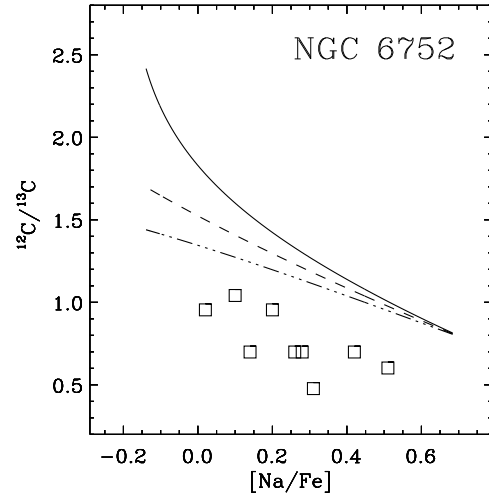


Figure 15. Carbon isotopic ratio $^{12}C/^{13}C$ versus $[Na/Fe]$ for the NGC 6752 reference model, plotted against the observational dataset of Yong et al. (2003). The dashed and dot-dashed lines represent a model in which the possible contribution of low metallicity, fast rotators are qualitatively taken into account according to Chiappini et al. (2008).

fast rotators gives very high values of the $^{12}C/^{13}C$ ratio of up to 10^4 because SNe II mainly produce ^{12}C (solid line in Fig. 15). Such high values are not reached in Fig. 15 because of the partial contribution from intermediate-mass AGB stars, that also produce low $^{12}C/^{13}C$ ratio yields (see Table 4). The Chiappini et al. (2008) model with rapidly rotating massive stars brings the ratio down to $^{12}C/^{13}C \sim 80$ (dashed line) at $[Fe/H] = -3.5$ and down to $^{12}C/^{13}C \sim 30$ (dot-dashed line) at $[Fe/H] = -5.0$. If low-metallicity, rapidly rotating massive stars contribute some ^{13}C , the predicted carbon isotope ratio will be lower but not as low as required to match the observational data (see dashed and dot-dashed line in Fig. 15).

Evidently it is not possible to reproduce the observed $^{12}C/^{13}C$ ratios without invoking internal stellar evolution (e.g., the first dredge-up and/or extra-mixing processes). In the more luminous sub-giant stars the observed isotopic ratio $^{12}C/^{13}C$ is very low, typically in the range of ~ 3 to 11 (noting that the equilibrium value of the CNO cycle is ≈ 3). The first dredge-up can reduce the ratio from 90 (solar) to ~ 20 in standard stellar evolution models (e.g., Boothroyd & Sackmann 1999). Shetrone (2003) found that in NGC 6528 and M 4 this ratio declines steeply with increasing luminosity along the RGB. The discontinuity in the $^{12}C/^{13}C$ ratio occurs at the bump luminosity and has also been detected in metal-poor field halo stars (Gratton et al. 2004).

Carretta et al. (2005) inferred a lower limit of 10 for the $^{12}C/^{13}C$ ratio for the three dwarf stars in NGC 104. Even if these values are more in accordance with our model, further determinations of the $^{12}C/^{13}C$ ratio in turn-off stars is needed before making a more detailed comparison.

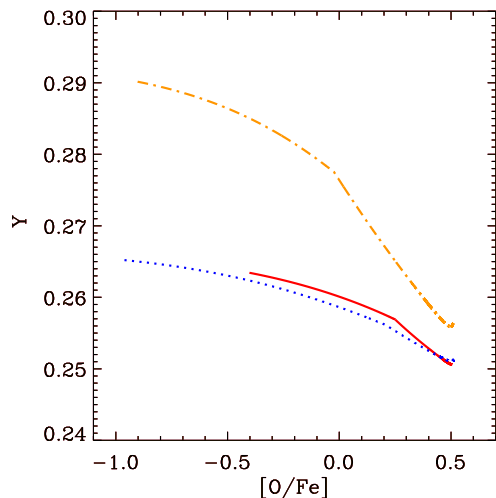


Figure 16. Evolution of the helium content, Y , versus $[O/Fe]$. The red solid line represents the model for NGC 6752; the blue dotted line for M 13; the dot dashed orange line for NGC 2808.

5.8 The Helium Content

The unusual HB morphology observed in NGC 2808, which exhibits an extended blue tail and a gap separating the red and the blue clumps (Bedin et al. 2000), can be reproduced if the blue stars have a higher helium content ($Y \sim 0.32$) compared to those in the red clump, with primordial helium ($Y \sim 0.24$) (D’Antona & Caloi 2004). NGC 2808 is also known to have a peculiar main sequence (D’Antona et al. 2005), in which the bluer stars are inferred to have a higher helium content from fitting theoretical isochrones to the observed data. To reproduce the colour-magnitude diagram (CMD), D’Antona et al. (2005) suggested that $\sim 20\%$ of the stars have a helium content as high as $Y \sim 0.40$, $\sim 30\%$ have a spread of Y between 0.24 and 0.29, while the remaining 50% of the stellar population have primordial Y . Further observations discovered a triple main sequence in NGC 2808 (Piotto et al. 2005), that has given support to the extreme value of $Y \sim 0.40$ required to fit the CMD.

Even if such large Y values are required to reproduce the main features of the CMD, the origin of the helium is not known. Helium values as high as $Y = 0.40$ are very difficult to reproduce with canonical chemical evolution models without violating other observational constraints (e.g. Karakas et al. 2006a). D’Antona & Caloi (2004) required a factor of ~ 10 more intermediate-mass AGB stars than what it is inferred from a Salpeter-like IMF to return the amount of Y needed to form the number of blue HB stars in NGC 2808. Karakas et al. (2006a) highlights the difficulty in producing the large postulated helium enrichment using the AGB self-pollution scenario. In particular, their largest predicted value of $Y \sim 0.29$ is accompanied by a large increase in sum C+N+O.

In Section 5.6 we show that one of the main successes of this model is the ability to reproduce the C+N+O sum for all three GCs NGC 6752, M 13, and NGC 2808. In Fig. 16 we plot the helium content Y of the reference models for each cluster against their $[O/Fe]$ abundances. Note that we

assume a primordial value of $Y \sim 0.248$ (Coc et al. 2004). It is quite evident that in the cases of NGC 6752 and M 13 the increase is quite modest and within $\Delta Y \sim 0.015$, whereas for the specific case of NGC 2808 we obtained $Y \sim 0.29$. This larger rise in the Y values is due to the larger density of polluting intermediate-mass AGB stars in NGC 2808, which is ~ 2 -3 times greater than for the other GCs.

Even if NGC 2808 is the only GC out of the three that shows a appreciable helium variation, a maximum value of $Y \sim 0.29$ is smaller than the postulated very high value of $Y \sim 0.40$ required to explain the most enriched stars in the triple main sequence (Piotto et al. 2007). It is very close, however, to the value of $Y \sim 0.32$ (Bedin et al. 2000) required to explain the unusual HB morphology for NGC 2808.

6 COMPARISON WITH PREVIOUS MODELS AND GENERAL COMMENTS

To explain the peculiar chemical properties observed in GCs, we propose a model based on a new idea of pre-peculiar inhomogeneous pollution produced by the explosion of a *single* SNe Ia. In principle, due to the low star formation rate during the formation of the proto-halo, the possibility that 2 or 3 (or more) SNe Ia explode essentially simultaneously (< 20 -30 Myr apart in time) in a region smaller than 30-50 pc is much less probable than having a single event. Having said that, our model can accommodate such a scenario without a dramatic impact on the predictions based upon the base scenario of a single SNe Ia event. For example, if 2 (or 3) SNe Ia explode in the same region, ejecting therefore a factor of 2 (or 3) more iron, an expansion (i.e., an increase of R_{in}) of a factor of $\sqrt[3]{2}$ (or $\sqrt[3]{3}$) would lead to the same $[Fe/H]$ and chemical properties seen in the base model. In the case of no SNe Ia, but intermediate-mass stellar AGB pollution, one is left with the classical “external” GC self enrichment scenario (Bekki et al. 2007) in which the high values of N, Na (and other elements produced in substantial amounts by AGB stars) are easily explained, but it is very difficult to explain the depletion in oxygen. Since all the well-observed GCs seem to have an oxygen-depleted population of stars at some level, in our framework we must assume that the inhomogeneous contribution of SN Ia is the *seed* for the formation of GCs.

Of course, a larger number of SNe Ia may contribute to the enrichment of the proto-halo ISM (outside the proto-GC region). We believe, though, that the approximation of an ISM being enriched only by SNII products is sound one, as the SNe Ia contribution to the “mean” MW’s stars’ chemical properties starts being important only after ~ 1.5 Gyr and at $[Fe/H] > -1$ (Tinsley 1979; Edvardsson et al. 1993; McWilliam 1997). The $[Fe/H]_{ISM}$ values in our models are, in all cases, lower than this value.

Bekki et al. (2007) point out that one of the greatest advantages of an external AGB-pollution scenario is that the fraction of peculiar stars observed in GCs is not limited to the amount of a stars forming in the first generation. In particular, in this model the fraction of O-depleted to O-rich stars depends only in the way that the SNe II pollution proceeds, while the number of AGB stars initially polluting the inner region is quite low ($N_{AGB} \simeq 200$; see Table 1). The total amount of stars needed to create a typical value of 200

intermediate-mass AGB stars is $\sim 10^4 M_{\odot}$, which is a small fraction of the total MW Halo or GC mass. Even assuming that this number of stars are trapped in the potential well of the forming GC and are homogeneously distributed within 50 (or 100) pc, their density would be 1.9×10^{-2} (2.4×10^{-3}) $M_{\odot} \text{pc}^{-3}$ which is low compared to the densities observed in GCs (e.g., Pryor & Meylan 1993).

In principle, our proposed scenario has no particular problems explaining the observed high fraction of peculiar to normal stars observed in some GCs (e.g., Carretta et al. 2006, for NGC 2808). The self-pollution scenario, on the other hand, requires ad hoc assumptions such as an anomalous IMF peaked at 4–8 M_{\odot} (e.g., Smith & Norris 1982; D’Antona & Caloi 2004; Prantzos & Charbonnel 2006); or that the GC was initially much more massive and has lost ~ 90 –99 per cent of the stars that were formed in the first generation through tidal stripping. Our model does not require these assumptions: the only assumption we require is that star formation should proceed more or less smoothly while SNe II explode and self enrich the proto-GC; and the chemical properties of the forming stars evolve from peculiar to normal. The fraction of normal to peculiar stars depends on how the SF proceeded and we will try to address this problem with detailed hydrodynamical simulations.

In previous models (e.g. Fenner et al. 2004; D’Antona et al. 2005; Bekki et al. 2007) the CN bimodality is not reproduced due to the lack of C-depleted and N-rich stars, since C is produced in AGB stars. The same is also true for Mg, with the result that positive C-N and Mg-Al correlations are found in contradiction to the observational constraints. Bekki et al. (2007) tried to solve this problem by using yields from AGB models that had no third dredge-up (as these authors noted, this assumption is purely hypothetical). The smaller production of C is what allows this study to reproduce the C-N anti-correlation. The O-Na and Al-Mg trends were not recovered because the lack of dredge-up resulted in a smaller production of Na and Mg (mainly ^{26}Mg). Note that in all AGB models, O destruction via HBB is not efficient enough to account for the very low O abundances observed in some GC stars (typically $[\text{O}/\text{Fe}] \approx -0.5$ or less). The non-standard models of Ventura & D’Antona (2005c) (see also Ventura & D’Antona 2006) that use a different convection model, can reproduce most of the abundance anomalies but only when including convective overshooting to force some third dredge-up along with adopting high mass-loss rates. In our model none of the above assumptions are required. We use the AGB yields of Karakas & Lattanzio (2007), averaged over a canonical Salpeter IMF.

The success of our model is the combined effect of inhomogeneous AGB pollution *together with* the effect of a single SN Ia and its Fe-rich ejecta. The net effect is to lower the ratio $[X_i/\text{Fe}]$, where the element X_i is negligibly produced (or destroyed) relative to SN II in intermediate-mass AGB stars (e.g., oxygen). In the case where X_i is produced by AGB stars, the ratio is either maintained at an approximately constant value or the enhancement is mitigated owing to the effect of the SN pollution (e.g., C, Na, Mg and possibly Al). The only real problem that our model suffers is the production of Al should be enhanced by a factor of ~ 10 –50 compared to the AGB yields from Karakas & Lattanzio

(2007). Our model, however, is the first that has shown any promise at explaining the Mg isotopic ratios in GC stars.

One possibility in a canonical AGB self-pollution model is that the second generation of stars did not form from AGB-enriched material but these stars had their surfaces polluted by AGB winds (e.g., Dantona et al. 1983). In our framework the O-depleted stars obtain their abundances from SNe Ia pollution mixed with AGB material. We could imagine a similar surface pollution model as follows: after the first “normal” generation of stars have formed, self pollution by intermediate-mass AGB stars and SNe Ia (which has similar timescales; see Section 2) start inhomogeneously polluting the surface of stars. It would be difficult, however, to explain all the chemical properties of GC stars with surface pollution. For example, it would probably not be possible to maintain $[\text{Fe}/\text{H}]$ constant in the most O-depleted stars. While surface pollution of SN Ia ejecta would decrease the $[\text{O}/\text{Fe}]$ ratio it would also dramatically increase the surface Fe content of the star.

7 CONCLUSIONS

We have modelled the chemical evolution of GCs under the hypothesis that the abundance anomalies were set during the formation of the Milky Way Halo (or inside their host dwarf galaxies). Inside a volume of gas enriched to some level by a first generation of low-metallicity SNe II, GC formation takes place owing to the inhomogeneous (respect to the surrounding ISM) effect of a single SN Ia plus material from intermediate-mass AGB stars. After a burst of star formation, new SNe II start to explode, self-polluting and expanding out the inhomogeneous region, which mixes with the surrounding (metal poorer) ISM. In our framework, all the peculiar stars observed in GCs (e.g., O-depleted, Na-rich) were born in the above inhomogeneously enriched volume, while “normal” stars (i.e., O-rich, Na-depleted) are formed successively once the SNe II associated with the SF have washed out the inhomogeneous region and self-polluted the ISM. In conclusion, our main findings can be summarized as follows:

(i) We reproduce the O-Na anti-correlation. In our model the first stars to form have low $[\text{O}/\text{Fe}]$ and high $[\text{Na}/\text{Fe}]$ abundances, with the system then evolving toward “normal” abundances once SNe II start polluting the ISM.

(ii) We reproduce the Mg-Al anti-correlation, but only by assuming that intermediate-mass AGB produce more Al than predicted by theoretical models (e.g., Karakas & Lattanzio 2007). This assumption needs to be carefully studied in the context of AGB model uncertainties.

(iii) We satisfactorily produce the Mg isotopic ratios observed in NGC 6752.

(iv) The $[\text{Fe}/\text{H}]$ abundance remains approximately constant during the evolution. This is because of mixing caused by the subsequent SNe II explosions between the Fe-enriched inhomogeneous inner region and the $[\text{Fe}/\text{H}]$ -poorer ISM. The Fe produced by the SNe II themselves does not significantly affect the resulting Fe abundance in the forming GC stars.

(v) We reproduce the C-N anti-correlation within observational uncertainties, and the sum C+N+O remains \approx constant, in agreement with the observations. The best fit is ob-

tained, however, by assuming that the AGB stars produce a factor of four less C. This assumption may not be in accord with current theoretical models.

(vi) The model cannot reproduce the $^{12}\text{C}/^{13}\text{C}$ ratios observed in evolved giant stars in the GCs, and internal stellar evolution processes are required.

(vii) GCs are a factor of \sim ten more metal rich than coeval MW halo stars (which are the assumed stellar host population).

In a forthcoming paper we will focus on other elements (e.g. Li, F, Si, Ca, Ti, V, Co, Ni, and Cu) to further test our framework. We will also focus upon the extreme metallicity GC cases that may prove to be a challenge for our model: the very metal poor M15 ($[\text{Fe}/\text{H}]=-2.26$) and the metal-rich 47 Tuc ($[\text{Fe}/\text{H}]=-0.76$). Preliminary results are encouraging.

One last question we could ask is why would all GCs show such a peculiar enrichment as outlined in this paper? Even if we do not have a conclusive answer, the region enriched by the SN Ia and AGB stars has a $[\text{Fe}/\text{H}]$ abundance and metallicity, Z , that is a factor of \sim ten higher than the surrounding ISM. Thus could be due to the corresponding enhanced cooling, this region may be more likely than the halo field to produce a star cluster with regions of enhanced star formation. In our framework, the SN Ia (and AGB) pollution is the seed which may have led to the formation of the globular cluster itself.

ACKNOWLEDGMENTS

We thank the anonymous referee whose comments improved the presentation of the paper. We also thank Eugenio Carretta and Maurizio Salaris for useful discussions regarding GC chemical abundances and isochrone, respectively. It is also a pleasure to thank Annibale D'Ercole for reading the paper and providing useful suggestions which improved the presentation of the paper. BKG acknowledges the support of the UK's Science & Technology Facilities Council (ST/F002432/1) and the Commonwealth Cosmology Initiative. AIK thanks Onno Pols for useful discussions and acknowledges support from the Australian Research Council's Discovery Projects funding scheme (DP0664105). PSB is supported by a Marie Curie Intra-European Fellowship within the 6th European Community Framework Programme.

REFERENCES

- Argast D., Samland M., Gerhard O. E., Thielemann F.-K., 2000, *A&A*, 356, 873
- Bedin L. R., Piotto G., Zoccali M., Stetson P. B., Saviane I., Cassisi S., Bono G., 2000, *A&A*, 363, 159
- Bekki K., Campbell S. W., Lattanzio J. C., Norris J. E., 2007, *MNRAS*, 377, 335
- Bekki K., Freeman K. C., 2003, *MNRAS*, 346, L11
- Bekki K., Norris J. E., 2006, *ApJ*, 637, L109
- Bemmerer D., Confortola F., Costantini H., Formicola A., Gyürky G., Bonetti R., Brogini C., Corvisiero P., Elekes Z., Fülöp Z., Gervino G., Guglielmetti A., Gustavino C., Imbriani G., Junker M., Laubenstein M., Lemut A., Limata B., Lozza V., Marta M., Menegazzo R., Prati P., Roca V., Rolfs C., Alvarez C. R., Somorjai E., Straniero O., Strieder F., Terrasi F., Trautvetter H. P., 2006, *Physical Review Letters*, 97, 122502
- Bonifacio P., Pasquini L., Molaro P., Carretta E., François P., Gratton R. G., James G., Sbordone L., Spite F., Zoccali M., 2007, *A&A*, 470, 153
- Boothroyd A. I., Sackmann I.-J., 1999, *ApJ*, 510, 232
- Briley M. M., Cohen J. G., Stetson P. B., 2004a, *AJ*, 127, 1579
- Briley M. M., Harbeck D., Smith G. H., Grebel E. K., 2004b, *AJ*, 127, 1588
- Brown J. H., Burkert A., Truran J. W., 1991, *ApJ*, 376, 115
- , 1995, *ApJ*, 440, 666
- Carretta E., Bragaglia A., Gratton R. G., Leone F., Recio-Blanco A., Lucatello S., 2006, *A&A*, 450, 523
- Carretta E., Bragaglia A., Gratton R. G., Lucatello S., Momany Y., 2007, *A&A*, 464, 927
- Carretta E., Gratton R. G., Lucatello S., Bragaglia A., Bonifacio P., 2005, *A&A*, 433, 597
- Cescutti G., 2008, *A&A*, 481, 691
- Charbonnel C., 1994, *A&A*, 282, 811
- , 1995, *ApJ*, 453, L41+
- Chiappini C., Ekström S., Meynet G., Hirschi R., Maeder A., Charbonnel C., 2008, *A&A*, 479, L9
- Chieffi A., Limongi M., 2004, *ApJ*, 608, 405
- Cioffi D. F., McKee C. F., Bertschinger E., 1988, *ApJ*, 334, 252
- Coc A., Vangioni-Flam E., Descouvemont P., Adahchour A., Angulo C., 2004, *ApJ*, 600, 544
- Cohen J. G., Briley M. M., Stetson P. B., 2002, *AJ*, 123, 2525
- Cohen J. G., Meléndez J., 2005, *AJ*, 129, 303
- Cottrell P. L., Da Costa G. S., 1981, *ApJ*, 245, L79
- D'Antona F., Bellazzini M., Caloi V., Pecci F. F., Galletti S., Rood R. T., 2005, *ApJ*, 631, 868
- D'Antona F., Caloi V., 2004, *ApJ*, 611, 871
- Dantona F., Gratton R., Chieffi A., 1983, *Memorie della Societa Astronomica Italiana*, 54, 173
- D'Antona F., Ventura P., 2007, *MNRAS*, 379, 1431
- Decressin T., Meynet G., Charbonnel C., Prantzos N., Ekström S., 2007, *A&A*, 464, 1029
- Denissenkov P. A., Herwig F., 2003, *ApJ*, 590, L99
- Denissenkov P. A., Tout C. A., 2000, *MNRAS*, 316, 395
- D'Ercole A., Vesperini E., D'Antona F., McMillan S. L. W., Recchi S., 2008, *MNRAS*, 391, 825
- Dopita M. A., Smith G. H., 1986, *ApJ*, 304, 283
- Fenner Y., Campbell S., Karakas A. I., Lattanzio J. C., Gibson B. K., 2004, *MNRAS*, 353, 789
- Fenner Y., Gibson B. K., Limongi M., 2002, *Ap&SS*, 281, 537
- Freeman K., Bland-Hawthorn J., 2002, *ARA&A*, 40, 487
- García-Hernández D. A., García-Lario P., Plez B., D'Antona F., Manchado A., Trigo-Rodríguez J. M., 2006, *Science*, 314, 1751
- Gibson B. K., Loewenstein M., Mushotzky R. F., 1997, *MNRAS*, 290, 623
- Gnedin O. Y., Zhao H., Pringle J. E., Fall S. M., Livio M., Meylan G., 2002, *ApJ*, 568, L23
- Goswami A., Prantzos N., 2000, *A&A*, 359, 191
- Gratton R., Sneden C., Carretta E., 2004, *ARA&A*, 42, 385

- Gratton R. G., Lucatello S., Bragaglia A., Carretta E., Cassisi S., Momany Y., Pancino E., Valenti E., Caloi V., Claudi R., D'Antona F., Desidera S., François P., James G., Moehler S., Ortolani S., Pasquini L., Piotto G., Recio-Blanco A., 2007, *A&A*, 464, 953
- Gratton R. G., Sneden C., Carretta E., Bragaglia A., 2000, *A&A*, 354, 169
- Grundahl F., Briley M., Nissen P. E., Feltzing S., 2002, *A&A*, 385, L14
- Harris W. E., 1996, *AJ*, 112, 1487
- Hughes G. L., Gibson B. K., Carigi L., Sánchez-Blázquez P., J.M. C., Lambert D. L., 2008, *MNRAS*, 390, 1710
- Ishimaru Y., Wanaajo S., 1999, *ApJ*, 511, L33
- Ivans I. I., Sneden C., Kraft R. P., Suntzeff N. B., Smith V. V., Langer G. E., Fulbright J. P., 1999, *AJ*, 118, 1273
- Iwamoto K., Brachwitz F., Nomoto K., Kishimoto N., Umeda H., Hix W. R., Thielemann F.-K., 1999, *ApJS*, 125, 439
- Izzard R. G., Lugaro M., Karakas A. I., Iliadis C., van Raai M., 2007, *A&A*, 466, 641
- James G., François P., Bonifacio P., Carretta E., Gratton R. G., Spite F., 2004, *A&A*, 427, 825
- Jehin E., Magain P., Neuforge C., Noels A., Thoul A. A., 1998, *A&A*, 330, L33
- Johnson C. I., Kraft R. P., Pilachowski C. A., Sneden C., Ivans I. I., Benman G., 2005, *PASP*, 117, 1308
- Karakas A., Lattanzio J. C., 2007, *Publications of the Astronomical Society of Australia*, 24, 103
- Karakas A. I., Fenner Y., Sills A., Campbell S. W., Lattanzio J. C., 2006a, *ApJ*, 652, 1240
- Karakas A. I., Lattanzio J. C., 2003, *Publications of the Astronomical Society of Australia*, 20, 279
- Karakas A. I., Lee H. Y., Lugaro M., Görres J., Wiescher M., 2008, *ApJ*, 676, 1254
- Karakas A. I., Lugaro M. A., Wiescher M., Görres J., Ugalde C., 2006b, *ApJ*, 643, 471
- Kobayashi C., Umeda H., Nomoto K., Tominaga N., Ohkubo T., 2006, *ApJ*, 653, 1145
- Kraft R. P., 1994, *PASP*, 106, 553
- Kraft R. P., Sneden C., Langer G. E., Shetrone M. D., 1993, *AJ*, 106, 1490
- Majewski S. R., Patterson R. J., Dinescu D. I., Johnson W. Y., Ostheimer J. C., Kunkel W. E., Palma C., 2000, in *Liege International Astrophysical Colloquia*, Noels A., Magain P., Caro D., Jehin E., Parmentier G., Thoul A. A., eds., p. 619
- Mannucci F., Della Valle M., Panagia N., 2006, *MNRAS*, 370, 773
- Marcolini A., D'Ercole A., Battaglia G., Gibson B. K., 2008, *MNRAS*, 386, 2173
- Marcolini A., D'Ercole A., Brighenti F., Recchi S., 2006, *MNRAS*, 371, 643
- Marcolini A., Sollima A., D'Ercole A., Gibson B. K., Ferraro F. R., 2007, *MNRAS*, 382, 443
- Marigo P., Bernard-Salas J., Pottasch S. R., Tielens A. G. G. M., Wesselius P. R., 2003, *A&A*, 409, 619
- Marino A. F., Villanova S., Piotto G., Milone A. P., Momany Y., Bedin L. R., Medling A. M., 2008, *A&A*, 490, 625
- Matteucci F., Recchi S., 2001, *ApJ*, 558, 351
- Melioli C., de Gouveia Dal Pino E. M., 2004, *A&A*, 424, 817
- Meynet G., Maeder A., 2002a, *A&A*, 390, 561
- , 2002b, *A&A*, 381, L25
- Morgan S., Lake G., 1989, *ApJ*, 339, 171
- Parmentier G., 2004, *MNRAS*, 351, 585
- Parmentier G., Gilmore G., 2001, *A&A*, 378, 97
- Parmentier G., Jehin E., Magain P., Neuforge C., Noels A., Thoul A. A., 1999, *A&A*, 352, 138
- Pasquini L., Bonifacio P., Molaro P., François P., Spite F., Gratton R. G., Carretta E., Wolff B., 2005, *A&A*, 441, 549
- Pinsonneault M., 1997, *ARA&A*, 35, 557
- Piotto G., Bedin L. R., Anderson J., King I. R., Cassisi S., Milone A. P., Villanova S., Pietrinferni A., Renzini A., 2007, *ApJ*, 661, L53
- Piotto G., Villanova S., Bedin L. R., Gratton R., Cassisi S., Momany Y., Recio-Blanco A., Lucatello S., Anderson J., King I. R., Pietrinferni A., Carraro G., 2005, *ApJ*, 621, 777
- Prantzos N., Charbonnel C., 2006, *A&A*, 458, 135
- Pryor C., Meylan G., 1993, in *Astronomical Society of the Pacific Conference Series*, Vol. 50, *Structure and Dynamics of Globular Clusters*, Djorgovski S. G., Meylan G., eds., pp. 357–+
- Rakos K., Schombert J., 2005, *PASP*, 117, 245
- Recchi S., Danziger I. J., 2005, *A&A*, 436, 145
- Romano D., Matteucci F., Tosi M., Pancino E., Bellazzini M., Ferraro F. R., Limongi M., Sollima A., 2007, *MNRAS*, 69
- Schaller G., Schaerer D., Meynet G., Maeder A., 1992, *A&AS*, 96, 269
- Shetrone M. D., 2003, *ApJ*, 585, L45
- Slavin J. D., Cox D. P., 1992, *ApJ*, 392, 131
- Smith G., 1996, *PASP*, 108, 176
- Smith G. H., 2006, *PASP*, 118, 1225
- Smith G. H., Norris J., 1982, *ApJ*, 254, 594
- Smith G. H., Norris J. E., 1993, *AJ*, 105, 173
- Smith G. H., Tout C. A., 1992, *MNRAS*, 256, 449
- Smith V. V., Cunha K., Ivans I. I., Lattanzio J. C., Campbell S., Hinkle K. H., 2005, *ApJ*, 633, 392
- Smith V. V., Suntzeff N. B., Cunha K., Gallino R., Busso M., Lambert D. L., Straniero O., 2000, *AJ*, 119, 1239
- Sneden C., Kraft R. P., Guhathakurta P., Peterson R. C., Fulbright J. P., 2004, *AJ*, 127, 2162
- Sweigart A. V., Mengel J. G., 1979, *ApJ*, 229, 624
- Thornton K., Gaudlitz M., Janka H.-T., Steinmetz M., 1998, *ApJ*, 500, 95
- Thoul A., Jorissen A., Goriely S., Jehin E., Magain P., Noels A., Parmentier G., 2002, *A&A*, 383, 491
- Timmes F. X., Woosley S. E., Weaver T. A., 1995, *ApJS*, 98, 617
- Tsujimoto T., Shigeyama T., Suda T., 2007, *ApJ*, 654, L139
- Ventura P., D'Antona F., 2005a, *A&A*, 431, 279
- , 2005b, *A&A*, 439, 1075
- , 2005c, *ApJ*, 635, L149
- , 2006, *A&A*, 457, 995
- Weiss A., Denissenkov P. A., Charbonnel C., 2000, *A&A*, 356, 181
- Wood P. R., Bessell M. S., Fox M. W., 1983, *ApJ*, 272, 99
- Woosley S. E., Weaver T. A., 1995, *ApJS*, 101, 181
- Yong D., Aoki W., Lambert D. L., 2006a, *ApJ*, 638, 1018
- Yong D., Aoki W., Lambert D. L., Paulson D. B., 2006b, *ApJ*, 639, 918

Yong D., Grundahl F., Lambert D. L., Nissen P. E.,
Shetrone M. D., 2003, *A&A*, 402, 985

Yong D., Grundahl F., Nissen P. E., Jensen H. R., Lambert
D. L., 2005, *A&A*, 438, 875

Yong D., Lambert D. L., Paulson D. B., Carney B. W.,
2008, *ApJ*, 673, 854